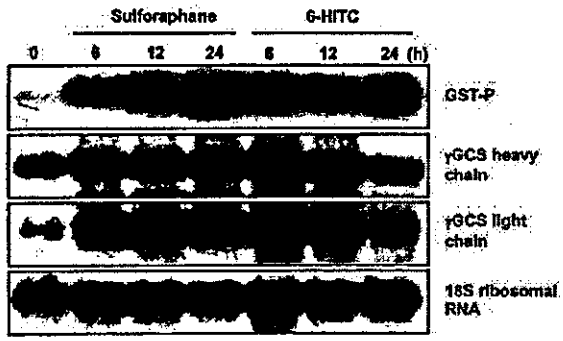

FIG. 6. **Induction of phase II enzyme gene expression by 6-HITC and sulforaphane.** The cells were treated with 5 μM 6-HITC and sulforaphane for different time intervals as indicated in the figures. 18S ribosomal mRNA represents the control to demonstrate that equal amounts of mRNA were probed in the Northern blot analysis.

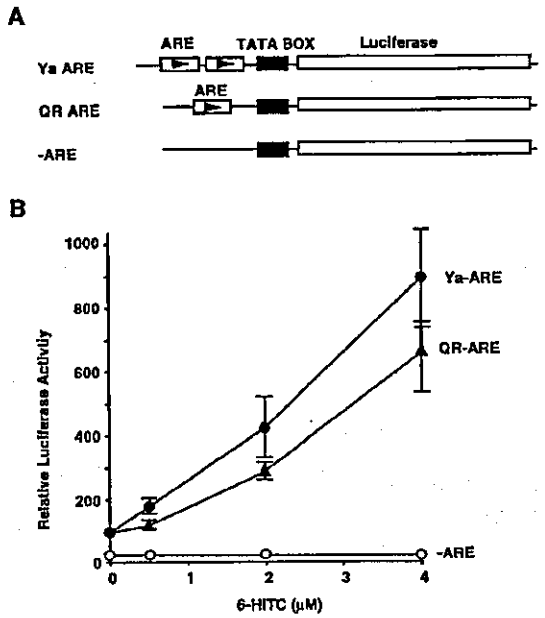

FIG. 7. **Activation of ARE reporter genes by 6-HITC.** *A*, structures of constructs used for transfections. *B*, time-dependent activation of ARE reporter genes by 6-HITC. Either pGSTA1-Luc, pNQO1-Luc, or pRBGP3 reporter plasmids were transfected into RL-34 cells. After transfection, the medium was changed to fresh medium, and the cells were treated with Me_2SO or 5 μM 6-HITC. Luc activity of the each reporter transfection in the absence of the chemical reagents was arbitrarily set to 1 and the mean values of three independent experiments, each carried out in duplicate, are shown with the standard error of the means (S.E.).

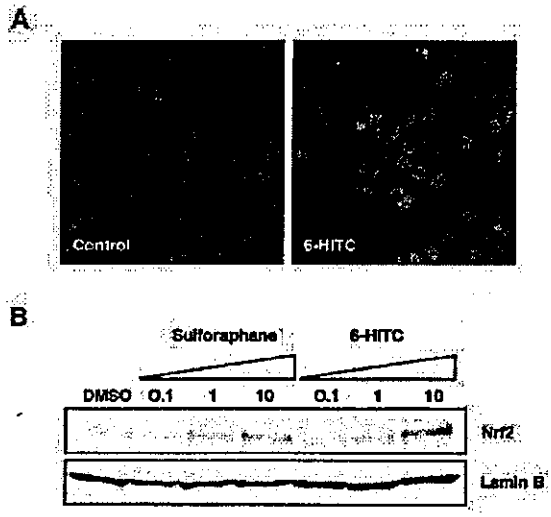

FIG. 8. **Activation of Nrf2.** *A*, induction of nuclear translocation of Nrf2 by 6-HITC. Panels: *A*, untreated control; *B*, 2 h after 6-HITC treatment. The RL34 cells were fixed in 2% paraformaldehyde and 0.2% picric acid and immunostained with anti-Nrf2 antibody. Images of the cellular immunofluorescence were acquired using a confocal laser scanning microscope. *B*, 6-HITC induces Nrf2 protein accumulation in the RL34 cells. Lamin B represents a control to demonstrate that equal amounts of proteins were probed in the immunoblot analysis.

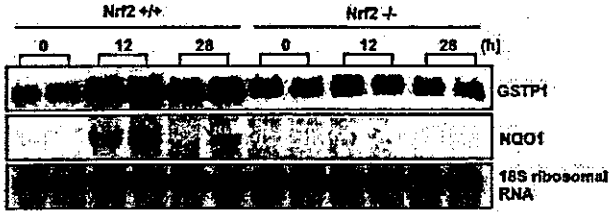

FIG. 9. **6-HITC induces phase II gene expression in mouse liver in an Nrf2-dependent manner.** Either the wild-type (*lanes 1-6*) or nrf2 (−/−) mice were treated with 6-HITC for the indicated periods.

zymes, the *nrf2*-deficient mice were exposed to the isothiocyanates, and the induction of the phase II enzyme gene expression was examined. The mRNA levels of the hepatic GSTP1, NQO1, and γ-GCS heavy chain and light chain were measured 28 h after a single administration of 6-HITC (15 μmol) or vehicle to female wild-type and *nrf2*-disrupted mice. As shown in Fig. 9, the mRNA levels of phase II enzymes were significantly increased by treatment with 6-HITC, while this induction was completely abrogated in the *nrf2*-deficient mice. Taken together, these data suggest that 6-HITC induces the ARE-mediated gene expression of the phase II enzymes via a Nrf2-dependent mechanism.

DISCUSSION

Epidemiological studies have demonstrated that the consumption of cruciferous vegetables is associated with a lower incidence of cancers (29–31). An important group of compounds that have this property are organosulfur compounds, such as the isothiocyanates. The isothiocyanates are compounds that occur as glucosinolates in a variety of cruciferous vegetables, such as *Brussica* species. Glucosinolates are found in the cell vacuoles of various plants in the family Cruciferae such as horseradish, mustard, broccoli, and wasabi. When plant cells are damaged, glucosinolates are hydrolyzed by myrosinase (thioglucoside glucohydrolase, EC 3.2.3.1), which is also produced in the same family, and produce isothiocyanates. It is known that wasabi contains isothiocyanate components, such as allyl isothiocyanate, 6-HITC, 7-methylthioheptyl isothiocyanate, and 8-methylthiooctyl isothiocyanate (32). These isothiocyanates have been suggested to have important medical benefits. They not only inhibit microbes, but can also help treat or prevent blood clotting and asthma (33). Many isothiocyanates are also effective chemoprotective agents against chemical carcinogenesis in experimental animals. The isothiocyanates have been shown to inhibit rat lung, esophagus, mammary gland, liver, small intestine, colon, and bladder tumorigenesis (34–37). It has been suggested that the anticarcinogenic effects of isothiocyanates are closely associated with their capacity to induce phase II detoxification enzymes and to inhibit phase I enzymes that are required for the bioactivation of carcinogens. Indeed, some of the isothiocyanates have been shown to inhibit cytochrome P450 and increase the carcinogen excretion or detoxification by the phase II detoxification enzymes (38–40).

Many natural isothiocyanates derived from cruciferous vegetables and some fruits have been shown to induce phase II enzymes in cultured cells and rodents (41–43). Recently, sulforaphane has been isolated from broccoli as the major inducer of phase II enzymes with potent *in vivo* chemopreventive properties (6, 14, 15). In addition, sulforaphane was found to inhibit the cytochrome P450 isozyme 2E1, which is responsible for the activation of a variety of genotoxic chemicals (43).

On the basis of its structural similarity to sulforaphane, the GST-inducing potencies of 6-HITC and sulforaphane were anticipated to be equally potent. However, the structure-activity relationship study revealed that the inducing potencies of 6-HITC was significantly greater than that for sulforaphane (Fig. 2). This was also the case in the animal experiments, in which the hepatic GST activity was induced more potently by 6-HITC than by sulforaphane (Fig. 5). The structure-activity relationship study also indicated that the isothiocyanate moiety is essential for the induction of GST activity (Fig. 2). Talalay *et al.* (7) have suggested that the inductive ability of various alkyl and aromatic isothiocyanates dependent on the presence of one hydrogen on the adjacent carbon to the isothiocyanate group and that tautomerization of the methylene-isothiocyanate moiety to a structure resembling an α, β-unsaturated thioketone may be important for inductive activity. However, the present study demonstrated that the methylthioalkyl isothiocyanates were less potent inducers than their *S*-oxidized forms (Fig. 2). The methylsulfinyl group, in addition to the isothiocyanate group, of 6-HITC is therefore suggested to be involved in its inductive activity. Although the reduced potency of the methylthioalkyl isothiocyanates may be simply due to their high volatility, it is not unlikely that the electron-withdrawing potentials of both the sulfinyl or sulfonyl groups may affect the signaling mechanism in the phase II induction.

To confirm that 6-HITC is absorbed into the body following its oral administration, the plasma level of 6-HITC and/or its GSH adduct was analyzed by the cyclocondensation assay, which provides a valid measurement of isothiocyanates or their dithiocarbamates, *i.e.* GSH derivatives (23). As shown in Fig. 4, it was revealed that 6-HITC was utilized very rapidly, reaching a maximum level within 30 min. Thus, 6-HITC is absorbed and rapidly enters the circulatory system. The plasma concentration of the isothiocyanate began to decrease after 30 min; however, this decrease was relatively slow. Zhang and Talalay (23) have recently proposed that the induction of phase II enzymes by isothiocyanates depends on their intracellular levels of accumulation in the cells. Therefore, the prolonged accumulation of 6-HITC in the circulatory system may also correlate with its phase II inducer potencies.

It is notable that 6-HITC specifically accelerated the production of GSTA1 and GSTP1 isozymes *in vitro* and *in vivo* (Figs. 3 and 5). The increase in GST activity by treatment with 6-HITC may, therefore, be largely attributable to the elevated synthesis of these isozymes. The class α GSTs represent the most abundant GST isozymes in the liver and kidney. It has been shown that a small increase in the class α GSTs is linked to a 90% decrease in the levels of the DNA adduct formation with aflatoxin B1, a liver carcinogen that is specifically detoxified by these isozymes (44). A recent study using transgenic mice lacking the class π GSTP1 has demonstrated that this class of GST is also involved in the metabolism of carcinogens, such as 7,12-dimethylbenz[*a*]anthracene, in mouse skin and has a profound effect on tumorigenicity (4). These data suggest that both isozymes may represent the important determinants in cancer susceptibility, particularly in diseases where exposure to polycyclic aromatic hydrocarbons is involved.

In early studies of the stress response system, a wide variety of phase II detoxification enzymes inducers were found to be electrophiles. Although the primary target of 6-HITC is still unknown, there is evidence that the intracellular level of GSH, regulating the redox state of the cell, may be an important sensor for the initiation of the cellular response to various compounds. In fact, the intracellular GSH levels of RL34 cells were readily reduced by treatment with 6-HITC.[2] Interestingly, the amount of GSH began to recover and increased to over the basal level, indicating that the cell responded to the GSH depletion. Because GSH is important in metabolism and enzyme regulation as well as the detoxification of cytotoxic materials, the level of intracellular GSH is a critical parameter for a signaling cascade for the induction of phase II enzymes by 6-HITC. On the other hand, it has also been shown that the gene expression of GSTA1 is related to the intracellular oxidative stress presumably mediated by reactive oxygen species or the pro-oxidative potential of GSTA1 inducers (45, 46). In addition to GSTA1, oxidative stress has been reported to enhance the expression of genes encoding other antioxidant enzymes, including the γ-GCS (47), heme oxygenase (48), and heat shock protein 90 (49). Thus, it is increasingly recognized that an adequate amount of oxidative stress stimulates a variety of signal transduction pathways under circumstances that do not result in cell death.

The transcriptional activation of the phase II enzymes has been traced to a *cis*-acting transcriptional enhancer called ARE (26), or alternatively, the electrophile response element (27). It has been shown that the transcription factor Nrf2 positively regulates the ARE-mediated expression of the phase II detoxification enzyme genes. Itoh *et al.* (24) have recently established by gene-targeted disruption in mice that Nrf2 is a general regulator of the phase II enzyme genes in response to electrophiles and reactive oxygens. More recently, the general regulatory mechanism underlying the electrophile counterattack response has been demonstrated in which electrophilic agents alter the interaction of Nrf2 with its repressor protein (Keap1), thereby liberating Nrf2 activity from repression by Keap 1, culminating in the induction of the phase II enzyme genes and antioxidative stress protein genes *via* AREs (28). It has been suggested that the dissociation of Nrf2 from Keap I may involve modification of either one of these proteins and could be achieved by direct or indirect mechanisms. For example, Nrf2 can be phosphorylated by components of the MAP kinase cascade (50), which could result in its dissociation. On the other hand, Dinkova-Kostova *et al.* (51) have provided an alternative possibility that the dissociation of this complex may be potentiated by the direct interaction of electrophilic agents with reactive thiol residues in either of the two proteins. This hypothesis is supported by the strong relationship between the potency of the agents as inducers of the gene expression through the ARE and their rate of reaction with sulfhydryl groups. This mechanism implies that the inducing agent will become covalently bound either to Keap I or Nrf2. Thus, our findings that (i) 6-HITC induced a significant increase in specific binding to the ARE (Fig. 7), (ii) 6-HITC activated Nrf2 (Fig. 8), and (iii) negligible inducibility in *nrf2*-deficient mice was observed (Fig. 9) suggest that 6-HITC may directly or indirectly act on the Keap 1/Nrf2 complex and activate ARE.

In conclusion, to identify novel cancer chemopreventive agents from plants, we screened extracts from a variety of commonly consumed vegetables on the basis of the GST-inducing effect and found that wasabi, which is known to have a variety of medical benefits, including the prevention of blood

[2] Y. Morimistu, Y. Nakagawa, and K. Uchida, unpublished observation.

clotting, asthma, and even cancer, was the richest source of inducers. An analysis of the wasabi extracts demonstrated that 6-HITC, the major isothiocyanate compound in wasabi, is the principal GST inducer. Moreover, we established the GST inducing potency of this compound not only *in vitro* but also *in vivo*. These and the previous findings that 6-HITC has an inhibitory effect on the growth of human stomach tumor cells and on skin carcinogenesis of mice induced by 12-*O*-tetradecanoylphorbol-13-acetate (52) suggested that this isothiocyanate may be a chemoprotector against tumors evoked by a number of chemical carcinogens and can be regarded as a readily available promising new cancer chemopreventive agent.

Acknowledgments—We thank G. Inoue (Kinjirushi Wasabi Co. Ltd.) for providing us all kinds of wasabi research samples.

REFERENCES

1. Hayes, J. D. & Pulford, D. J. (1995) *CRC Crit. Rev. Biochem. Mol. Biol.* **30**, 445–600
2. Wattenberg, L. W. (1983) *Cancer Res.* **43**, 2488–2493
3. Wattenberg, L. W. (1985) *Cancer Res.* **45**, 1–8
4. Henderson, C. J., Smith, A. G., Ure, J., Brown, K., Bacon, E. J. & Wolf, C. R. (1998) *Proc. Natl. Acad. Sci. U. S. A.* **95**, 5275–5280
5. Nakae, D., Denda, A., Kobayashi, Y., Akai, H., Kishida, H., Tsujiuchi, T., Konishi, Y., Suzuki, T. & Muramatsu, M. (1998) *Jpn. J. Cancer Res.* **89**, 1118–1125
6. Prestera, T., Holtzclaw, W. D., Zhang, Y. & Talalay, P. (1993) *Proc. Natl. Acad. Sci. U. S. A.* **90**, 2965–2969
7. Talalay, P., De Long, M. J. & Prochaska, H. J. (1988) *Proc. Natl. Acad. Sci. U. S. A.* **85**, 8261–8265
8. Spencer, S. R., Xue, L., Klenz, E. M. & Talalay, P. (1991) *Biochem. J.* **273**, 711–717
9. Colditz, G. A., Branch, L. G., Lipinick, R. J., Willett, W. C., Rosner, B., Posner, B. M. & Hennekens, C. H. (1985) *Am. J. Clin. Nutr.* **41**, 32–36
10. Graham, S. (1983) *Cancer Res.* **43**, 2409–2413
11. Peto, R., Doll, R., Buckley, J. D. & Sporn, M. B. (1981) *Nature* **290**, 201–208
12. Wattenberg, L. W., Sparnins, V. L. & Barany, G. (1989) *Cancer Res.* **49**, 2689–2692
13. Prochaska, H. J., Santamaria, A. B. & Talalay, P. (1992) *Proc. Natl. Acad. Sci. U. S. A.* **89**, 2394–2398
14. Zhang, Y., Talalay, P., Cho, C.-G. & Posner, G. H. (1992) *Proc. Natl. Acad. Sci. U. S. A.* **89**, 2399–2403
15. Zhang, Y., Kensler, T. W., Cho, C.-G., Posner, G. H. & Talalay, P. (1994) *Proc. Natl. Acad. Sci. U. S. A.* **91**, 3147–3150
16. Kawamoto, Y., Nakamura, Y., Naito, Y., Torii, Y., Kumagai, T., Osawa, T., Ohigashi, H., Satoh, K., Imagawa, M. & Uchida, K. (2000) *J. Biol. Chem.* **275**, 11291–11299
17. Etoh, H., Nishimura, A., Takasawa, R., Yagi, A., Saito, K., Sakata, K., Kishima, I. & Ina, K. (1990) *Agric. Biol. Chem.* **54**, 1587–1591
18. Habig, W. H., Pabst, M. J. & Jakoby, W. B. (1974) *J. Biol. Chem.* **249**, 7130–7139
19. Prochaska, H. J. & Santamaria, A. B. (1988) *Anal. Biochem.* **169**, 328–336
20. Kennedy, S. W., Lorenzen, A., James, C. A. & Collins, B. T. (1993) *Anal. Biochem.* **211**, 102–112
21. Ishii, T., Itoh, K., Takahashi, S., Sato, H., Yanagawa, T., Katoh, Y., Bannai, S. & Yamamoto, M. (2000) *J. Biol. Chem.* **275**, 16023–16029
22. Igarashi, K., Kataoka, K., Itoh, K., Hayashi, N., Nishizawa, M. & Yamamoto, M. (1994) *Nature* **367**, 568–572
23. Zhang, Y. & Talalay, P. (1988) *Cancer Res.* **58**, 4632–4639
24. Itoh, K., Chiba, T., Takahashi, S., Ishii, T., Igarashi, K., Katoh, Y., Oyake, T., Hayashi, N., Satoh, K., Hatayama, I., Yamamoto, M. & Nabeshima, Y. (1997) *Biochem. Biophys. Res. Comm.* **236**, 313–322
25. Morimitsu, Y., Hayashi, K., Nakagawa, Y., Horio, F., Uchida, K. & Osawa, T. (2000) *Biofactors* **13**, 271–276
26. Rushmore, T. H., King, R. G., Paulson, K. E. & Pickett, C. B. (1990) *Proc. Natl. Acad. Sci. U. S. A.* **87**, 3826–3830
27. Friling, R. S., Bensimon, A., Tichauer, T. & Daniel, V. (1990) *Proc. Natl. Acad. Sci. U. S. A.* **87**, 6258–6262
28. Itoh, K., Wakabayashi, N., Katoh, Y., Ishii, T., Igarashi, K., Engel, J. D. & Yamamoto, M. (1999) *Gene Dev.* **13**, 76–86
29. Lee, H. P., Gourley, L., Duffy, S. W., Esteve, J., Lee, J. & Day, N. E. (1989) *Int. J. Cancer* **434**, 1007–1016
30. Olsen, G. W., Mandel, J. S., Gibson, R. W., Wattenberg, L. W., and Schuman, L. M. (1991) *Cancer Causes Control* **2**, 291–297
31. Mehta, B. G., Liu, J., Constantinou, A., Thomas, C. F., Hawthorne, M., You, M., Gerhauser, C., Pezzuto, J. M., Moon, R. C. & Moriarty, R. M. (1995) *Carcinogenesis* **16**, 399–404
32. Ina, K., Ina, H., Ueda, M., Yagi, A. & Kishima, I. (1989) *Agric. Biol. Chem.* **53**, 537–538
33. Depree, J. A., Howard, T. M. & Savage, G. P. (1999) *Food Res. Inter.* **31**, 329–337
34. Wattenberg, L. W. (1981) *Cancer Res.* **41**, 2991–2994
35. Morse, M. A., Zu, H., Galati, A. J., Schmidt, C. J. & Stoner, G. D. (1993) *Cancer Lett.* **72**, 103–110
36. Stoner, G. D., Morrissey, D. T., Heur, Y. H., Daniel, E. M., Galati, A. J. & Wagner, S. A. (1991) *Cancer Res.* **51**, 2063–2068
37. Hecht, S. S. (1995) *J. Cell. Biochem. Suppl.* **22**, 195–209
38. Talalay, P. (1989) *Adv. Enzyme Regul.* **28**, 237–250
39. Guo, Z., Smith, T. J., Wang, E., Eklind, K., Chung, F.-L. & Yang, C. S. (1993) *Carcinogenesis* **14**, 1167–1173
40. Morse, M. A. & Stoner, G. D. (1993) *Carcinogenesis* **14**, 1737–1746
41. Leonard, T. B., Popp, J. A., Graichen, M. E. & Dent, J. G. (1981) *Carcinogenesis* **2**, 473–482
42. Yang, C. S., Smith T. J., and Hong, J. Y. (1994) *Cancer Res.* **54**, 1982–1986
43. Barcelo, S., Gardiner, J. M., Gescher, A. & Chipman, J. K. (1996) *Carcinogenesis* **17**, 277–282
44. Hayes, J. D., Judah, D. J., McLellan, L. I., Kerr, L. A., Peacock, S. D. & Neal, G. E. (1991) *Biochem. J.* **279**, 385–398
45. Pinkus, R., Weiner, L. M. & Daniel, V. (1995) *Biochemistry* **34**, 81–88
46. Pinkus, R., Weiner, L. M. & Daniel, V. (1996) *J. Biol. Chem.* **271**, 13422–13429
47. Shi, M. M., Kugelman, A., Iwamoto, T., Tian, L. & Forman, H. J. (1994) *J. Biol. Chem.* **269**, 26512–26517
48. Lautier, D., Luscher, P. & Tyrrell, R. M. (1992) *Carcinogenesis* **13**, 227–232
49. Fukuda, A., Osawa, T., Oda, H., Tanaka, T., Toyokuni, S. & Uchida, K. (1996) *Biochem. Biophys. Res. Commun.* **219**, 76–81
50. Yu, R., Lei, W., Mandlekar, S., Weber, M. J., Der, C. J., Wu, J. & Kong, A.-N. T. (1999) *J. Biol. Chem.* **274**, 27545–27552
51. Dinkova-Kostova, A. T., Massiah, M. A., Bozak, R. E., Hicks, R. J. & Talalay, P. (2001) *Proc. Natl. Acad. Sci. U. S. A.* **98**, 3404–3409
52. Fuke, Y., Haga, Y., Ono, H., Nomura, T. & Ryoyama, K. (1997) *Cytotechnology* **25**, 197–203

Carcinogenesis vol.23 no.3 pp.457–462, 2002

Nrf2 transactivator-independent GSTP1-1 expression in 'GSTP1-1 positive' single cells inducible in female mouse liver by DEN: a preneoplastic character of possible initiated cells

Kimihiko Satoh[1,6], Ken Itoh[2], Masayuki Yamamoto[2], Masanori Tanaka[3], Makoto Hayakari[4], Keizou Ookawa[4], Takehiko Yamazaki[4], Tsuyoshi Sato[1], Shigeki Tsuchida[4] and Ichiro Hatayama[5]

[1]Department of Medical Technology, Hirosaki University, School of Health Science, Hon-Cho 66-1, Hirosaki 036-8564, [2]Institute of Basic Medical Sciences and Center for TARA, University of Tsukuba, Tennoudai, Tsukuba 305, [3]Second Department of Pathology, Hirosaki University, School of Medicine, Hirosaki 036-8562, [4]Second Department of Biochemistry, Hirosaki University, School of Medicine, Hirosaki 036-8562 and [5]Aomori Prefectural Institute of Health and Environment, Higashi-Tsukurimichi 1-1-1, Aomori 030-0913, Japan

[6]To whom correspondence should be addressed
Email: kisatoh@cc.hirosaki-u.ac.jp

Whether single cells immunohistochemically positive for glutathione *S*-transferase P1-1 (GSTP1-1) induced in the female mouse liver by DEN (Hatayama *et al., Carcinogenesis*, 14, 537–538, 1993) are precursor initiated cells of preneoplastic foci, is of importance in chemical hepatocarcinogenesis. Nrf2 transactivates a wide variety of ARE (antioxidant response element)-mediated enzymes including GSTP1-1. Quantitative examination revealed that the basal expression of hepatic GSTP1-1 was 60% lower in Nrf2 gene knock-out female mice$^{-/-}$ than in wild type females, and that treatment with butyrated hydroxyanisole (BHA) increased by 10-fold GSTP1-1 expression in the liver of wild type female mice but not in knockout female mice$^{-/-}$. Despite the lack of Nrf2, GSTP1-1-positive single cells were detected in livers of DEN-treated female$^{-/-}$ 3 months after treatment. Subsequent BHA feeding to the positive cell-bearing females for one more week clearly showed that the single cells were detectable with females$^{-/-}$ but not with females$^{+/+,+/-}$ due to the strong induction of GSTP1-1 in the surrounding hepatocytes. The sensitivity to DEN hepatocarcinogenesis was not significantly different among genotypes. These results demonstrate that Nrf2 is regulatory in normal hepatocytes but not in the single cells positive for GSTP1-1 inducible in the female mouse liver by DEN. The transcriptional distinction observed for the DEN-transformants is suggestive of a preneoplastic character of precursor initiated cells.

Introduction

Whether single cells immunohistochemically positive for glutathione *S*-transferase P1-1 (GSTP1-1) induced in the rat and mouse livers by DEN (1–3) are precursor initiated cells of preneoplastic foci (4,5), remains to be elucidated. The Pi class GST is one of the most up-regulated enzymes in preneoplastic and neoplastic cells in various mammalian species (6–9). We were the first to demonstrate that injection of a single dose of diethylnitrosamine (DEN) results in the appearance of single cells and mini-foci heavily positive for GST-P (GSTP1-1) in the rat liver within 48 h of injection (1,2). Similar cells have also been detected in the liver of female mouse by us (3). Based on the phenotypic identity and other features, the DEN-transformant cells are considered to be precursors of preneoplastic foci (1–3,10). In order to characterize the possible initiated cells further, the mouse expression system is advantageous for several reasons. For example, the single cell populations are stably and reproducibly detectable in female livers over a period of >3 months. As a matter of course, gene knockout technology is applicable to the experimental animal system.

The GSTP1-1 expression can be tentatively classified into two types; a specific induction in preneoplastic and neoplastic cells by chemical carcinogens, and non-specific induction by non-carcinogenic agents such as anti-oxidants (7,8). In fact, GSTP1-1 is overexpressed in the normal male liver, and its concentration is ~10-fold higher than in the female liver. The Pi class species is inducible in the female up to the level seen in males following 1–2 weeks treatment with the antioxidant BHA (12–14). The enzyme level also changes markedly upon castration (15–17).

The 5′-upstream regions of the genes of the Pi class species of rat, mouse, and human, are fairly different to each other indicating that these marker species are similar but differently regulated under physiological conditions (19–21). The transactivating factor Nrf2 (NFE-2 related factor 2), which belongs to the leucine zipper (bZip) transcription factor family, has been implicated as a key molecule involved in ARE (antioxidant response element)-mediated gene expression of enzymes and proteins, especially phase II drug-metabolizing enzymes including glutathione *S*-transferases (15–17).

In an attempt to determine the characteristics of GSTP1-1-positive single cells, we used quantitative assays to examine the regulatory roles of Nrf2 with the gene-disrupted animals. Specifically, we examined the basal and inductive expression of GSTA3-3, GSTM1-1 and GSTP1-1, induction of GSTP1-1-positive single cells, and the response to the carcinogenic agent DEN in Nrf2 knockout mice.

Abbreviations: BHA, 3(2)-*t*-butyl-4-hydroxyanisole; DEN, *N,N*-diethynitrosamine; GSTP1-1, glutathione *S*-transferase (GST) P1-1 species; single cells, GSTP1-1 positive single cells.

Materials and methods

Chemicals

DEN, BHA, 2,4-dinitro-1-chlorobenzene (CDNB), and 1,2-dichloro-4-nitrobenzene (DCNB), were purchased from Wako Chemical Co. (Tokyo). All other chemicals were obtained from commercial sources and were of high reagent grade.

Animals and diets

Nrf2-disrupted male and female mice were prepared as reported previously (20) and wild type CD-1 mice, aged 5 weeks, were obtained from CLEA (Tokyo). The animals were maintained at the Institute for Animal Experiments of Hirosaki University and all animal experiments followed the Guidelines for Animal Experimentation of Hirosaki University.

Assays for glutathione-S-transferases

GSTs were assayed using CDNB, DCNB and ethacrynic acid as substrates in 100 mM Na_2HPO_4, pH 6.5 at 25°C, using the method described by Habig *et al.* (22). Cumene hydroperoxidase was assayed as described by Wendel (23).

Table I Hepatic GST activities in male and females of Nrf2-gene disrupted mice

	Enzyme activity (units/g.w.w.)			
	CDNB[a]	GSTA3-3[b]	GSTM1-1[c]	GSTP1-1[d]
Males				
+/+	772 ± 133 (100 ± 17.2)	38.4 ± 6.3 (100 ± 16.4)	11.2 ± 1.8 (100 ± 16.1)	55.0 ± 11.2 (100 ± 20.4)
+/−	464 ± 103 (60.1 ± 13.3)	36.0 ± 4.7 (93.7 ± 13.1)	4.25 ± 0.4 (37.9 ± 3.6)	45.5 ± 3.8 (82.7 ± 6.9)
−/−	268 ± 55 (34.7 ± 7.2)	24.8 ± 2.5 (64.5 ± 10.3)	1.03 ± 0.16 (9.2 ± 1.4)	31.3 ± 3.8 (56.9 ± 6.9)
Females				
+/+	205 ± 35.7 (100 ± 17.4)	38.2 ± 6.4 (100 ± 16.9)	5.6 ± 0.67 (100 ± 21.6)	6.8 ± 1.2 (100 ± 17.6)
+/−	129 ± 71.8 (62.9 ± 35.0)	33.2 ± 2.2 (86.9 ± 6.6)	3.91 ± 1.06 (69.8 ± 18.9)	3.6 ± 0.7 (52.9 ± 10.3)
−/−	100 ± 6.0 (48.8 ± 3.0)	25.9 ± 1.0 (67.2 ± 4.1)	1.57 ± 0.25 (28.0 ± 4.6)	3.85 ± 0.52 (56.6 ± 7.6)

Isozymes were assayed in three to four mice in each group.
[a]Total activity assayed with CDNB; [b]cumene hydroperoxide activity; [c]DCNB activity; [d]ethacrynic acid activity.
Values are mean ± SD and those in parentheses are percentages, relative to the activity in the corresponding wild type.

Quantitation of GST isozymes

Antibodies against the three major forms, GSTA3-3, GSTM1-1, and GSTP1-1, were raised in rabbits and the protein content of each isozyme was quantitated by the single radial immunodiffusion method (SRID) as described previously (7,18).

DEN hepatocarcinogenesis

Nrf2-disrupted homozygous males$^{-/-}$ were mated with the heterozygous females$^{+/-}$ to obtain a number of hetero- and homozygotes (20). Newborn mice received a single intraperitoneal injection of DEN (10 mg/kg body wt) when 15 days old. The animals were fed basal diet *ad libitum* and killed at 3 and 6 months after treatment. The livers were quickly dissected and removed, and then fixed in ice-cold acetone.

Immunohistochemical staining

Immunohistochemical staining was carried out by the avidin–biotin–peroxidase complex (ABC) method (24).

Statistical analysis

All data were expressed as mean ± SEM. Differences between groups were examined for statistical significance using the Student's *t*-test.

Results

Hepatic GST isozyme expression in Nrf2-gene disrupted mice

Basal expression of hepatic GSTs. Hepatic GST levels in knockout$^{+/-, -/-}$ and wild type$^{+/+}$ mice were examined quantitatively by measuring enzymatic activity and protein content. GSTA3-3, GSTM1-1 and GSTP1-1 activities were assayed with specific substrates, cumene hydroperoxide, DCNB, and ethacrynic acid, respectively. In wild type animals, total CDNB activity in males was 3.9-fold greater than in females (Table I). This was mostly due to differences in GSTP1-1 activity. As shown in Figure 1, GSTP1-1 protein content in the male liver (5.1 ± 0.8 mg/g) was significantly higher than the other two forms. In contrast, the amount of GSTP1-1 (0.5 ± 0.1 mg/g) in females was significantly lower than those of the other two forms. The amounts of the two GSTs were relatively independent of sex.

Basal levels of the three GSTs in the Nrf2 gene-disrupted animal livers were generally lower than those in the wild type. Total GST activities in knockout males$^{-/-}$ and females$^{-/-}$ were 34.7 and 48.8% those of the males$^{+/+}$ and females$^{+/+}$, respectively. Furthermore, GSTA3-3 activities in knockout animals were 64.5 and 67.2% of those in the wild type males and females, respectively. Similarly, GSTP1-1 activity in the livers of knockout mice$^{-/-}$ was ~60% of that in the wild type for either sex. In contrast, GSTM1-1 activity and protein content in males$^{-/-}$ were as low as 9.2% and 7.9% of those in wild type males$^{+/+}$, respectively. Further comparison showed that the enzymatic activities in heterozygote animals$^{+/-}$ were

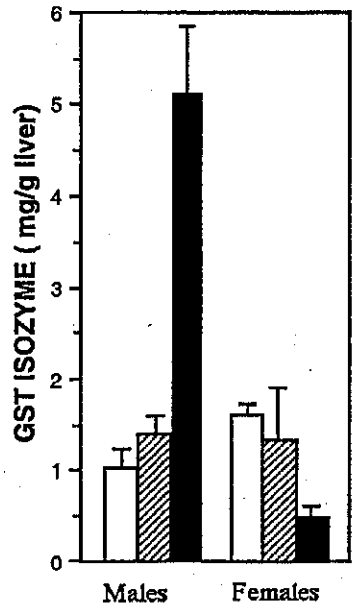

Fig. 1. Isozyme composition of three major GSTs in the liver of wild type male and female mice. □, GSTA3-3; ▨, GSTM1-1; ■, GSTP1-1.

intermediate between those of homozygotes$^{+/+}$ and homozygotes$^{-/-}$, where GSTA3-3 and GSTP1-1 activities in males$^{+/-}$ were similar to those in wild types$^{+/+}$ (Figure 2). Thus, the effects of Nrf2 gene disruption on the GST isozymes were in the order of GSTM1-1 >> GSTP1-1 > GSTA3-3 in males, and GSTM1-1 > GSTP1-1 > GSTA3-3 in females.

Effect of gene disruption on induction of hepatic GSTs in female mice by BHA. We next determined quantitatively the effects of Nrf2 gene disruption on the induction of hepatic GSTs in female knockout$^{+/+, +/-, -/-}$ and wild type mice treated with BHA for 12 days (12–14). As a measure of induction, we determined the percent increment in hepatic GSTs in BHA-treated animals relative to that in control mice (Figure 3A–E). Induction of total CDNB activity in knockout homozygotes$^{-/-}$ (250%) was significantly lower than in control wild$^{+/+}$ (850%) and heterozygotes$^{+/-}$ (950%) (Figure 3A). Furthermore, the expression levels of GSTM1-1 (Figure 3C) and GSTP1-1 (Figure 3D and E) in BHA-treated knockout homozygotes$^{-/-}$, but not GSTA3-3 expression (Figure 3B), were less than those in control wild$^{+/+}$ and knockout heterozygotes$^{+/-}$. Similarly,

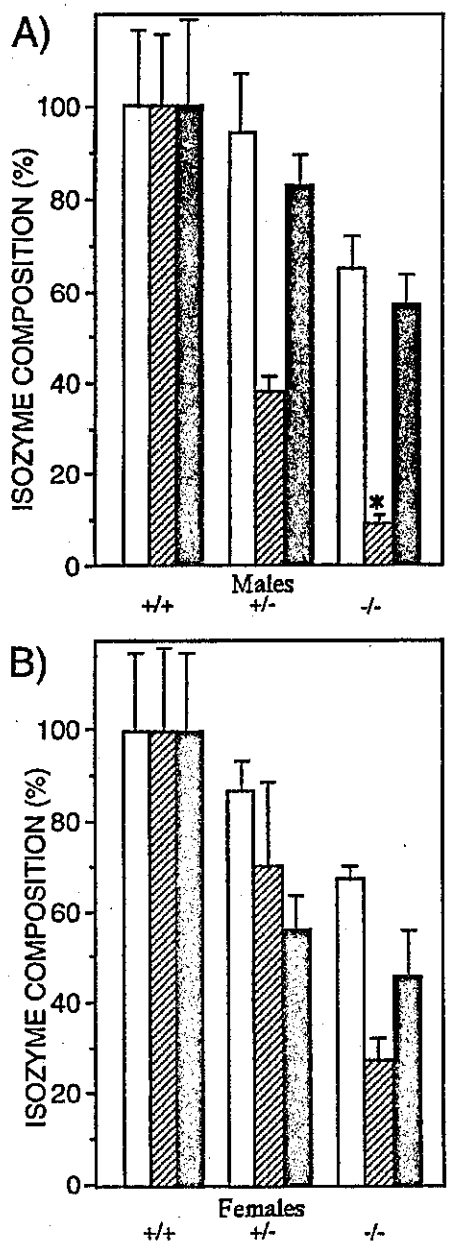

Fig. 2. Isozyme composition of three major GSTs in the liver of wild type and Nrf2-gene disrupted mice. (A) male mice; (B) female mice. □, GSTA3-3; ▨, GSTM1-1; ■, GSTP1-1. *9.2%.

while the levels of GSTP1-1 activity and protein increased by 340% and 530%, respectively, in BHA-treated wild type females$^{+/+}$ and as high as 810% and 1240%, respectively, in knockout heterozygote females, those levels were as low as 230% and 280%, respectively, in knockout animals$^{-/-}$ (Figure 3D and E). These results indicate that the expression levels of GSTs in the livers of the three genotypes were in order of (+/–) ≥ (+/+) >> (–/–).

DEN hepatocarcinogenesis in Nrf2-gene disrupted mice

Sensitivity to DEN in knockout females. The carcinogenic sensitivities of the three genotypic females (+/+, +/–, –/–) were examined according to the DEN hepatocarcinogenesis protocol (3). Multiple GSTP1-1 positive single cells were noted in the livers 3 months after injection of DEN, irrespective of genotype. However, mini-foci were not detected in these animals at that stage (Table II). There was no statistical correlation among the single cell populations induced in the liver of the three genotypes. After a longer period of 6 months, single cells were also abundantly induced in the livers of all animals, together with some mini-foci. Although the number of single cells in the liver of knockout mice$^{-/-}$ was apparently greater than that in wild type mice, the difference was weak ($P < 0.05$), and the difference with that in knockout heterozygotes was not statistically significant. Thus, the sensitivities of homozygote and heterozygote knockout female mice to the hepatocarcinogenic effect of DEN were not different from that of wild type animals.

Induction of GSTP1-1-positive single cells in knockout female$^{-/-}$, $^{+/-}$ livers and effect of subsequent BHA treatment. GSTP1-1-positive single cells were noted in the livers of Nrf2 gene disrupted female mice as well as in wild type females. In order to confirm the induction of minor cells, 0.75% BHA containing diet was subsequently fed to the single cell-bearing mice for one more week. As seen in the immunohistochemical staining patterns of control animal livers, hepatocytes strongly positive for GSTP1-1 were noted throughout the whole liver in control female mice$^{+/+}$ untreated and treated with BHA (Figure 4d and e), but not in the livers of knockout females$^{-/-}$ (Figure 4f). In DEN-treated females, GSTP1-1-positive single cells were detected in the livers of wild type$^{+/+}$ as well as in the knockout animals$^{-/-}$ (Figure 4g and h). However, while single cells were not detected in the wild type after treatment with BHA (Figure 4j and k), minor cell populations were detected in knockout mice$^{-/-}$ even after treatment with the anti-oxidant (Figure 4l). Immunohistochemical patterns of heterozygotes$^{+/-}$ were very similar to or identical with those of wild types as summarized in Figure 5. These results clearly indicate that Nrf2 plays a major role in the basal and induced expression of GST in normal hepatocytes but not in the expression of the marker species in 'GSTP1-1 positive' single cells.

Discussion

To further characterize the potentially preneoplastic cells, i.e. DEN-induced GSTP1-1-positive single cells in the livers of female mice (3), we quantitatively examined in the present study two aspects of the regulatory roles of Nrf2 transactivator in the expression of Pi class GST using Nrf2 gene disrupted mice. The first was the effect of gene disruption on the basal and induced expression of three hepatic GST isozymes. The second was the induction of GSTP1-1-positive single cells in the liver of knockout females$^{-/-}$ as well as the hepatocarcinogenic effect of DEN in knockout mice.

Effect of Nrf2 gene disruption on non-carcinogenic induction of hepatic GSTP1-1

Quantitative analysis showed that the effect of Nrf2 gene disruption on the basal expression of GSTs was most prominent on the basal expression of GSTM1-1 in the liver of male mice; the basal activity and protein content were <10% of the wild type males. Since Mu class GSTs are not tumor specific

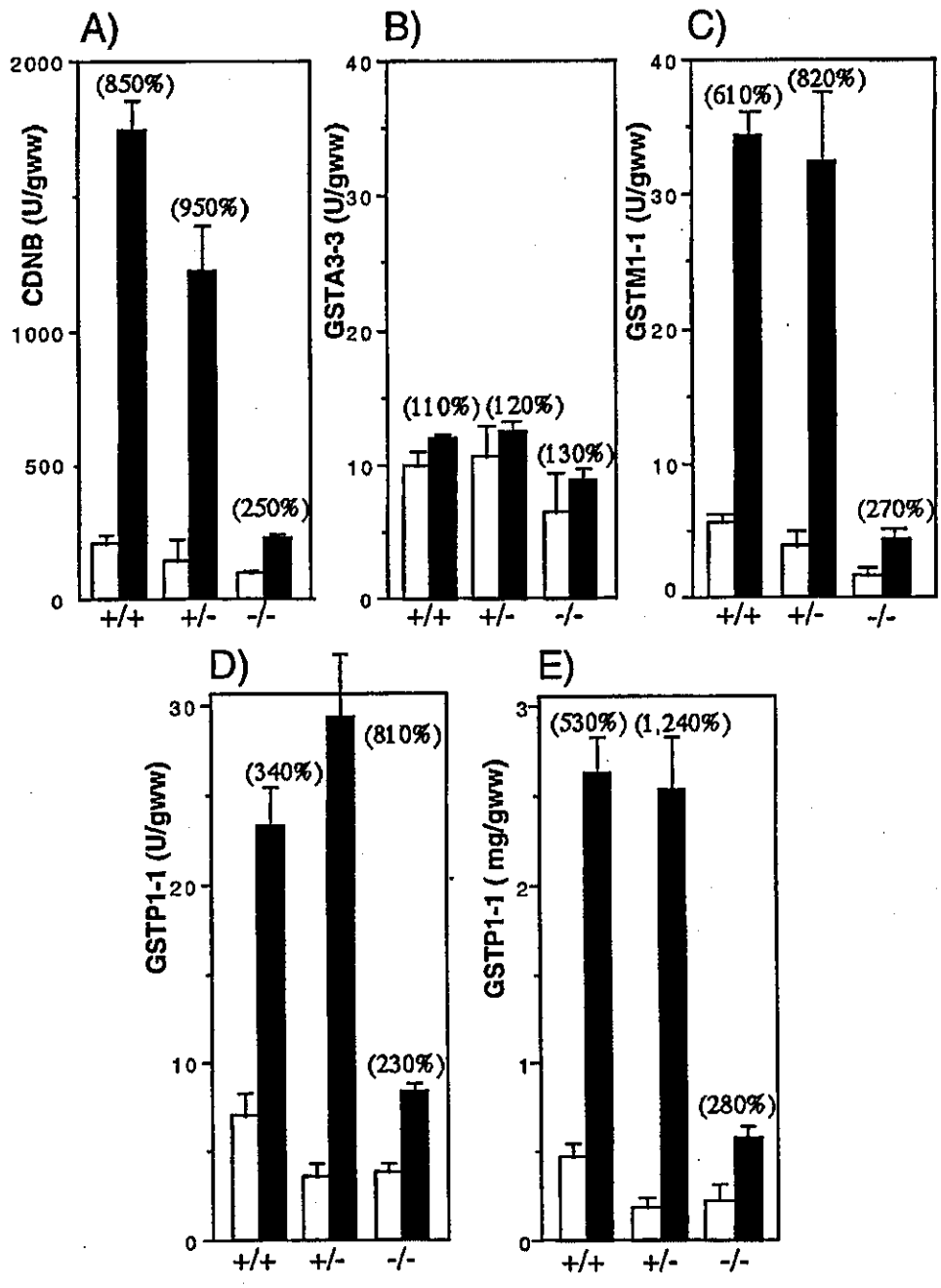

Fig. 3. Induction of three major GSTs in the liver of wild-type and Nrf2 gene knockout$^{+/+,-/-}$ female mice following administration of BHA. Open and shaded bars represent the amounts of hepatic GSTs in animals fed basal diet and 0.75% BHA-containing diet for 12 days, respectively. GST activities were assayed as described in Table I. GSTP1-1 protein was quantitated by the SRID method. Values in parentheses denote induction (%).

species and distinct ARE sequences are not detectable in the 5'-upstream regions of the GSTM1-1 genes (29), the results indicate that Nrf2 regulates tumor-specific isozyme species as well as non-tumor specific (or tissue-specific) isozymes. Apart from the significant effect on GSTM1-1 expression in males, Nrf2 transactivator accounted for ~40% of the basal expression of GSTP1-1 in the liver of either sex. The effect of gene disruption was much more marked on the induction of expression of hepatic GSTP1-1 than on the basal expression, as the expression of the isozyme was significantly low in knockout females$^{-/-}$, in agreement with the findings of Hayes *et al.* (25) and Ramos-Gomez *et al.* (26). Combined together, these results indicate that the role of Nrf2 in the induction of expression of GSTP1-1 is more important than the basal/constitutive expression of GSTP1-1 species in normal hepatocytes.

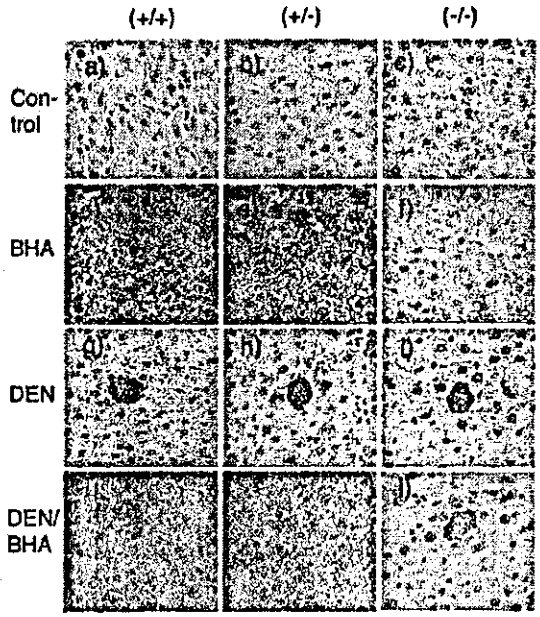

Fig. 4. Immunohistochemical GSTP1-1 staining patterns of livers of wild type and knockout female mice. BHA, 0.75%BHA feeding for 1 week; DEN, i.p. administration of DEN followed by feeding basal diet for 3 months; DEN/BHA, DEN treatment followed by BHA feeding. See also Figure 5.

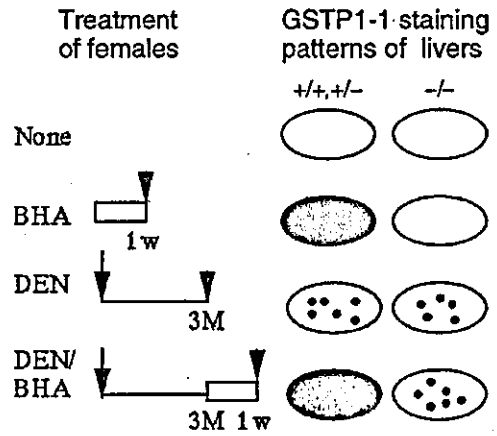

Fig. 5. Schematic diagram for the induction of GSTP1-1-positive single cells in the livers of wild type and Nrf2 gene knockout$^{-/-}$ female mice. Arrowheads denote time of examination. Open and solid circles represent GSTP1-1 negative and positive liver patterns, respectively, and small dots represent GSTP1-1-positive single cells.

Effect of Nrf2 on carcinogenic induction of GSTP1-1

That Nrf2 transcription factor is a major positive regulator of GSTP1-1 expression implies that homozygous and heterozygous knockout mice might be more sensitive to carcinogens than wild type$^{+/+}$, and that GSTP1-1-positive single cells and mini-foci might be undetectable in the female$^{-/-}$ livers in the early stages of DEN-induced hepatocarcinogenesis. However, no significant differences were observed in DEN carcinogenicity between homozygous and heterozygous female knockout mice, compared with those of wild type females. In addition, distinct GSTP1-1 positive single cell populations were induced in livers of homozygous and heterozygous female knockout mice as in those of wild type. The Nrf2-independent expression of the GSTP1-1-positive single cells was further confirmed by the subsequent treatment with BHA to single cell-bearing animals. As shown in the schematic diagram in Figure 5, no single cells were found in anti-oxidant treated heterozygous female knockout mice and wild type mice due to the strong induction of GSTP1-1 in the surrounding hepatocytes. In contrast, minor cell populations were detected in the livers of BHA-treated homozygous female knockout mice, in whom GSTP1-1 was hardly induced in normal hepatocytes. These results indicate that Nrf2 was involved in the regulation of the basal and induced expression of GSTP1-1 in normal hepatocytes but was not involved in the induction of 'GSTP1-1 positive' single cells, foci and nodules (adenomas) in mice treated with DEN. Single cells could, therefore, be differentiated from normal hepatocytes based on the genetic regulation of GSTP1-1 expression by the Nrf2 transcription factor. The transcriptional distinction could be another characteristic feature of the single cell populations, which does not contradict the biochemical and pathological data so far obtained (1–5), suggesting that these cells are precursors of preneoplastic foci and nodules (adenomas).

Table II. Single cells and mini-foci positive for GSTP1-1 induced in the liver of wild type and knockout female mice by DEN

	Single cells		Mini-foci		
Female mice	n^a	No. cm^2	No. cm^2	mm^2/cm^2	mm^2/focus
3 months-DEN					
+/+	4	33 ± 17	n.d.	n.d.	n.d.
+/−	6	69 ± 41	n.d.	n.d.	n.d.
−/−	9	66 ± 38	n.d.	n.d.	n.d.
6 months-DEN					
+/+	4	30 ± 11	0.3 ± 0.3	0.6 ± 0.1	1.0 ± 0
+/−	6	46 ± 19	1.4 ± 1.0	1.5 ± 1.1	1.2 ± 0.5
−/−	6	78 ± 37*	0.3 ± 0.5	0.6 ± 1.0	2.0 ± 0

[a]Number of animals examined. GSTP1-1 positive cells were estimated as described in Materials and methods. n.d., not detected. *$P < 0.05$, compared with wild type mice.

Previous studies showed that the Nrf2 transcription factor synergistically heterodimerizes with Small maf (MafG and MafK) or c-Jun on binding to ARE, as positive and negative regulators of the expression of various phase II detoxicating enzymes as well as other proteins (26–28). The present findings suggest that the process of induction of GSTP1-1 in the single cells (possible initiated cells) is not, however, related to Nrf2/Small maf/ARE-mediated ones, and is rather different from that in normal hepatocytes.

The above results suggest that Nrf2 protein could be one of the major transcription factors for GSTP1-1 expression, in addition to c-JUN and c-FOS (15–17,30). However, it is rather strange that these transactivators do not play major roles in the carcinogenic induction of GSTP1-1 (31). No significant oncogenic changes have so far been detected in preneoplastic cell populations in experimental animals except for some occasional activation of c-myc or H-ras (32–34). In this regard, Gijssel *et al.* (35) have also noted the lack of p53 protein expression in GSTP1-1 (GST-P)-positive preneoplastic foci and nodules in rats.

The present results suggest that GSTP1-1-positive single cells are formed to be preneoplastic cells, being transcriptionally distinct from normal hepatocytes. Are the single cell

populations initiated cells? What is the initial oncogenic change(s), if any, in these cells? These are important questions that need to be resolved to clarify the molecular and cellular events involved in the initiation stage of chemical hepatocarcinogenesis in experimental animals as pointed out earlier by Farber and Pitot, as well as by Prehn (4,5,36,37).

Acknowledgements

This work was supported in part by Grants-in-Aid for Cancer Research from the Ministry of Education, Science, Sports and Culture of Japan, Grants-in-Aid from the Intelligent Cosmos Academic Foundation (Sendai), and funds from NOF Corporation (Tokyo) and CHUGAI Pharmaceuticals (Tokyo).

References

1. Moore,M.A., Nakagawa,K., Satoh,K., Ishikawa,T. and Sato.K. (1987) Single GST-P positive liver cells–putative initiated hepatocytes. *Carcinogenesis*, 8, 483–486.
2. Satoh,K., Hatayama,I., Tateoka,N., Tamai,K., Shimizu,T., Tatematsu,M., Ito,N. and Sato,K. (1989) Transient induction of single GST-P positive hepatocytes by DEN. *Carcinogenesis*, 10, 2107–2111.
3. Hatayama,I., Nishimura,S., Narita,T. and Sato,K. (1993) Sex-dependent expression of class pi glutathione *S*-transferase during chemical hepatocarcinogenesis in B6C3F1 mice. *Carcinogenesis*, 14, 537–538.
4. Farber,E. (1980) The sequential analysis of liver cancer induction. *Biochim. Biophys. Acta*, 605, 149–166.
5. Pitot,H.C. (1985) Principles of carcinogenesis: chemical. In De Vita,V.T. Jr, Hellman,S. and Rosenburg,S.A. (eds) *Cancer: Principles and Practice of Oncology*. J.B. Lippincott, Philadelphia, PA, pp. 116–135.
6. Mannervik,B. and Danielson,U.H. (1988) Glutathione *S*-transferases; structure and catalytic activity. *CRC Crit. Rev. Biochem.*, 23, 283–337.
7. Satoh,K., Kitahara,A., Soma,Y., Inaba,Y., Hatayama,I. and Sato,K. (1985) Purification, induction, and distribution of placental glutathione transferase: A new marker enzyme for preneoplastic cells in the rat chemical hepatocarcinogenesis. *Proc. Natl Acad. Sci. USA*, 85, 3964–3968.
8. Sato,K. (1989) Glutathione transferases as markers of preneoplasia and neoplasia. *Adv. Cancer Res.*, 52, 205–255.
9. Rowe,J.D., Patskovsky,Y.V., Patskovska,L.N., Novikova,E. and Listowsky,I. (1998) Rationale for reclassification of a distinctive subdivision of mammalian class Mu glutathione *S*-transferases that are primarily expressed in testis. *J. Biol. Chem.*, 273, 9593–9601.
10. Schulte-Hermann,R., Timmermann-Trosiener,I. and Schuppler,J. (1983) Promotion of spontaneous preneoplastic cells in rat liver as a possible explanation of tumor production by nonmutagenic compounds. *Cancer Res.*, 43, 839–844.
11. Dragan,Y.P., Hully,J.R., Nakamura,J., Mass,M.J., Swenberg,J.A. and Pitot,H.C. (1994) Biochemical events during initiation of rat hepatocarcinogenesis. *Carcinogenesis*, 15, 1451–1458.
12. Benson,A.M., Batzinger,R.P., Ou,S.Y., Bueding,E., Cha.,Y.N. and Talalay,P. (1978) Elevation of hepatic glutathione *S*-transferase activities and protection against mutagenic metabolites of benzo(*a*)pyrene by dietary antioxidants. *Cancer Res.*, 38, 4486–4495.
13. Pearson,W.R., Reinhart,J., Sisk,S.C. and Anderson,K.S. (1988) Tissue-specific induction of murine glutathione transferase mRNAs by butylated hydroxyanisole. *J. Biol. Chem.*, 263, 13324–13332.
14. McLellan,L.I. and Hayes,J.D. (1989) Differential induction of class Alpha glutathione *S*-transferases in mouse liver by the anti-carcinogenic antioxidant butylated hydroxyanisole. *Biochem. J.*, 263, 393–402.
15. Okuda,A., Sakai,M. and Muramatsu,M. (1987) The structure of the rat glutathione *S*-transferase P gene and related pseudogenes. *J. Biol. Chem.*, 262, 3858–3863.
16. Bammler,T.K., Smith,C.A. and Wolf,C.R. (1994) Isolation and characterization of two mouse Pi-class glutathione *S*-transferase genes. *Biochem. J.*, 298, 385–90.
17. Morrow,C.S., Goldsmith,M.E. and Cowan,K.H. (1990) Regulation of human glutathione *S*-transferase pi gene transcription: influence of 5′-flanking sequences and trans-activating factors which recognize AP-1-binding sites. *Gene*, 88, 215–222.
18. Hatayama,I., Satoh,K. and Sato,K. (1986) Developmental and hormonal regulation of the major form of hepatic glutathione *S*-transferase in male mice. *Biochem. Biophys. Res. Commun.*, 140, 581–588.
19. Itoh,K., Chiba,T., Takahasi,S., Ishii,T. *et al.*(1997) An Nrf2/Small Maf heterodimer mediates the induction of Phase II detoxifying enzyme genes through antioxidant response elements. *Biochem. Biophys. Res. Commun.*, 236, 313–322.
20. Itoh,K., Wakabayashi,N., Katoh,Y., Ishii,T., Igarashi,K., Engel,J.D. and Yamamoto,M. (1999) Keap1 represses nuclear activation of antioxidant responsive elements by Nrf2 through binding to the amino-terminal Neh2 domain. *Genes Dev.*, 13, 76–86.
21. Nguyen,T., Huang,J.I.C. and Pickett,C.B. (2000) Transcriptional regulation of the antioxidant response element. Activation by Nrf2 and repression by MafK. *J. Biol. Chem.*, 275, 15466–15473.
22. Habig,W.H., Pabst,M.J. and Jakoby,W.B. (1974) Glutathione *S*-transferase. *J. Biol. Chem.*, 249, 7130–7139.
23. Wendel,A. (1981) Glutathione peroxidase. In Jakoby,W.B. (ed.) *Methods in Enzymology*. Academic Press, San Diego, Vol. 77, pp. 325–333.
24. Tatematsu,M., Mera,Y., Inoue,T., Satoh,K., Sato,K. and Ito,N. (1988) Relative merits of immunohistochemical demonstrations of placental, A, B and C forms of glutathione *S*-transferase and histochemical demonstration of gamma-glutamyl transferase as markers of altered foci during liver carcinogenesis in rats. *Carcinogenesis*, 8, 221–225.
25. Hayes,J.D., Chanas,S.A., Henderson,C.J, McMahon,M., Sun,C., Moffat,G.J., Wolf,C.R. and Yamamoto,M. (2000) The Nrf2 transcription factor contributes both to the basal expression of glutathione *S*-transferases in mouse liver and to their induction by the chemopreventive synthetic antioxidants, butylated hydroxyanisole and ethoxyquin. *Biochem. Soc. Trans.*, 28, 33–41.
26. Ramos-Gomez,M., Kwak,M.K., Dolan,P.M., Itoh,K., Yamamoto,M., Talalay,P. and Kensler,T.W. (2001) Sensitivity to carcinogenesis is increased and chemoprotective efficacy of enzyme inducers is lost in nrf2 transcription factor-deficient mice. *Proc. Natl Acad. Sci. USA*, 98, 3410–3415.
27. Wild,A.C., Moinova,H.R. and Mulcahy,R.T. (1999) Regulation of gamma-glutamylcysteine synthetase subunit gene expression by the transcription factor Nrf2. *J. Biol. Chem.*, 274, 33627–33636.
28. Dhakshinamoorthy,S. and Jaiswal,A.K. (2000) Small maf (MafG and MafK) proteins negatively regulate antioxidant response element-mediated expression and antioxidant induction of the NAD(P)H: Quinone oxidoreductase 1 gene. *J. Biol. Chem.*, 275, 40134–40141.
29. Reinhart,J. and Pearson,W. (1993) The structure of two murine Class-Mu transferase genes coordinately induced by butylated hydroxyanisole. *Arch. Biochem. Biophys.*, 303, 383–393.
30. Power,C., Sinha,S., Webber,C., Manson,M.M. and Neal,G.E. (1987) Transformation related expression of glutathione-*S*-transferase P in rat liver cells. *Carcinogenesis*, 8, 797–801.
31. Sakai,M., Okuda,A. and Muramatsu,M. (1988) Multiple regulatory elements and phorbol 12-O-tetradecanoate 13-acetate responsiveness of the rat placental glutathione transferase gene. *Proc. Natl Acad. Sci. USA*, 85, 9456–9460.
32. Suzuki,S., Satoh,K., Nakano,H., Hatayama,I., Sato,K. and Tsuchida,S. (1995) Lack of correlated expression between the glutathione *S*-transferase P-form and the oncogene products c-Jun and c-Fos in rat tissues and preneoplastic hepatic foci. *Carcinogenesis*, 16, 567–571.
33. Beer,D.G., Schwarz,M., Sawada,N. and Pitot,H.C. (1986) Expression of H-ras and c-myc protooncogenes in isolated gamma-glutamyl transpeptidase-positive rat hepatocellular carcinomas induced by diethylnitrosamine. *Cancer Res.*, 46, 2435–2441.
34. Butterworth,B.E., Sprankle,C.S., Goldsworthy,S.M., Wilson,D.M. and Goldsworthy,T.L. (1994) Expression of myc, fos, and Ha-ras in the livers of furan-treated F344 rats and B6C3F1 mice. *Mol. Carcinog.*, 9, 24–32.
35. Gijissel,H.E., Stenius,U., Mulder,G.J. and Meerman,J.H.N. (2000) Lack of p53 protein expression in preneoplastic rat hepatocytes *in vitro* after exposure to N-acetoxy-acetylaminofluorene, X-rays or a proteasome inhibitor. *Eur. J. Cancer*, 36, 106–112.
36. Prehn,R.T. (1994) Cancers beget mutations versus mutations beget cancers. *Cancer Res.*, 54, 5296–5300.
37. Farber, E. (1996) The step-by-step development of epithelial cancer: from phenotype to genotype. *Adv. Cancer Res.*, 70, 21–48.

Received July 31, 2001; revised November 12, 2001; accepted November 14, 2001

Role of NRF2 in Protection Against Hyperoxic Lung Injury in Mice

Hye-Youn Cho, Anne E. Jedlicka, Sekhar P. M. Reddy, Thomas W. Kensler, Masayuki Yamamoto, Liu-Yi Zhang, and Steven R. Kleeberger

Department of Environmental Health Sciences, The Bloomberg School of Hygiene and Public Health, Johns Hopkins University, Baltimore, Maryland; and Institute of Basic Medical Sciences and Center for Tsukuba Advanced Research Alliance, University of Tsukuba Tennoudai, Tsukuba, Japan

NRF2 is a transcription factor important in the protection against carcinogenesis and oxidative stress through antioxidant response element (ARE)-mediated transcriptional activation of several phase 2 detoxifying and antioxidant enzymes. This study was designed to determine the role of NRF2 in the pathogenesis of hyperoxic lung injury by comparing pulmonary responses to 95–98% oxygen between mice with site-directed mutation of the gene for NRF2 (*Nrf2*$^{-/-}$) and wild-type mice (*Nrf2*$^{+/+}$). Pulmonary hyperpermeability, macrophage inflammation, and epithelial injury in *Nrf2*$^{-/-}$ mice were 7.6-fold, 47%, and 43% greater, respectively, compared with *Nrf2*$^{+/+}$ mice after 72 h hyperoxia exposure. Hyperoxia markedly elevated the expression of NRF2 mRNA and DNA-binding activity of NRF2 in the lungs of *Nrf2*$^{+/+}$ mice. mRNA expression for ARE-responsive lung antioxidant and phase 2 enzymes was evaluated in both genotypes of mice to identify potential downstream molecular mechanisms of NRF2 in hyperoxic lung responses. Hyperoxia-induced mRNA levels of NAD(P)H:quinone oxidoreductase 1 (NQO1), glutathione-S-transferase (GST)-Ya and -Yc subunits, UDP glycosyl transferase (UGT), glutathione peroxidase-2 (GPx2), and heme oxygenase-1 (HO-1) were significantly lower in *Nrf2*$^{-/-}$ mice compared with *Nrf2*$^{+/+}$ mice. Consistent with differential mRNA expression, NQO1 and total GST activities were significantly lower in *Nrf2*$^{-/-}$ mice compared with *Nrf2*$^{+/+}$ mice after hyperoxia. Results demonstrated that NRF2 has a significant protective role against pulmonary hyperoxic injury in mice, possibly through transcriptional activation of lung antioxidant defense enzymes.

Reactive oxygen species (ROS) have been implicated in the pathogenesis of many acute and chronic pulmonary disorders such as adult respiratory distress syndrome and bronchopulmonary dysplasia (1). In laboratory animals, administration of pure oxygen (> 95%, hyperoxia) causes extensive pulmonary damage characterized by inflammation and death of capillary endothelial and alveolar epithelial cells resulting in pulmonary edema and severe impairment of respiratory functions (2, 3). Sufficiently long exposure (≥ 3 d) to hyperoxia is lethal to animals (4). The precise molecular mechanism(s) by which hyperoxia produces lung injury remain(s) unresolved. However, excess production of ROS that could overwhelm endogenous pulmonary antioxidant defense systems has been proposed (5), and a number of studies have focused on enzymatic defense components in the pathogenesis of oxygen-induced lung damage (6–13).

In laboratory rodents, hyperoxia causes increases of "classic" antioxidant enzymes (e.g., superoxide dismutase [SOD], glutathione peroxidase [GPx], glutathione reductase [GR], and catalase) in the lung (6, 7). The protective roles of these enzymes in the development of oxidative lung damage have been proposed in a few *in vivo* studies with genetically engineered mice (i.e., gene knockout mice and transgenic mice). For example, lung inflammation and damage was attenuated in mice that overexpressed SOD3, relative to wild-type (*wt*) mice (8); partial protection against hyperoxic lung injury was also observed in transgenic mice overexpressing SOD2 (9). Tsan and colleagues suggested that SOD2 gene-knockout mice were more susceptible to pulmonary hyperoxic injury than normal mice (10). Enhanced pulmonary antioxidant enzyme activity through exogenous administration of SOD1 and/or catalase also provided protection to rats against hyperoxic insults (11). Heme oxygenase-1 (HO-1), an oxidative stress protein, has been also shown to be protective in hyperoxic pulmonary injury (12, 13). In addition, phase 2 detoxifying enzymes including NAD(P)H:quinone oxidoreductase 1 (NQO1) and glutathione-S-transferase (GST) have attracted attention due to their protective roles against oxidative processes in malignant cells or tissues (14, 15). As indirect antioxidants, phase 2 enzymes detoxify reactive electrophilic metabolites, such as organic peroxides, lipid peroxides, epoxides, and quinones, and facilitate their excretion through conjugation reaction or two-electron reduction. However, little is known about the contribution of phase 2 detoxifying enzymes to lung defense against oxygen toxicity.

NF-E2–related factor 2 (NRF2) is a recently identified cap'n'collar basic leucine zipper transcription factor. It was originally detected in erythroid cells, but abundant NRF2 mRNA expression has subsequently been described in murine liver, intestine, lung, and kidney, where detoxification reactions occur routinely (16, 17). High similarity exists between the NRF2 binding sequence (NF-E2 consensus sequence) and antioxidant response element (ARE, also referred to as electophilic response element). Conse-

(*Received in original form January 16, 2001 and in revised form September 17, 2001*)

Address correspondence to: Steven R. Kleeberger, Ph.D., Laboratory of Pulmonary Pathobiology, National Institute of Environmental Health Sciences, National Institutes of Health, Research Triangle Park, NC 27709.

Abbreviations: antioxidant response element, ARE; bronchoalveolar lavage fluid, BALF; butylated hydroxyanisole, BHA; butylated hydroxytoluene, BHT; 1-chloro 2,4-dinitrobenzene, CDNB; α-dithiothreitol, DTT; ethylenediaminetetraacetic acid, EDTA; electrophoretic mobility shift assay, EMSA; flavine adenine dinucleotide, FAD; γ-glutamate cystein ligase regulatory subunit, GCLS; glutathione peroxidase, GPx; glutathione reductase, GR; glutathione-S-transferase, GST; N-[2-hydroxyethyl]piperazine-N'-[2-ethanesulfonic acid, HEPES; tris buffered EDTA, TBE; heme oxygenase-1, HO-1; 3-(N-morpholino)propanesulfonic, MOPS; nicotinamide adenine dinucleotide, reduced form, NADH; nuclear factor, erythroid 2, NF-E2; NAD(P)H:quinone oxidoreductase 1, NQO1; NF-E2–related factor 2, NRF2; ICR/Sv129 mice, *Nrf2*$^{+/+}$; ICR/Sv129 mice with site-directed mutation in *Nrf2*, *Nrf2*$^{-/-}$; polymorphonuclear leukocyte, PMN; phenylmethanesulfonyl fluoride, PMSF; polydeoxyinosinic-deoxycytidylic acid, polydI-dC; reactive oxygen species, ROS; reverse transcriptase polymerase chain reaction, RT-PCR; standard error of the mean, SEM; superoxide dismutase, SOD; UDP glycosyl transferase, UGT.

Am. J. Respir. Cell Mol. Biol. Vol. 26, pp. 175–182, 2002
Internet address: www.atsjournals.org

quently, NRF2 has induced mRNA expression for ARE-bearing phase 2 detoxifying enzymes such as NQO1, GST-Ya subunit, and γ-glutamate cysteine ligase regulatory subunit (GCLS), classic antioxidant enzymes (e.g., catalase, SOD1), and HO-1, and protected cells against carcinogenesis and oxidative stress in various *in vivo* (17–19) and *in vitro* (20–23) models. The role of NRF2 in the pathogenesis of oxygen toxicity, however, has not been studied in the lungs of laboratory animals.

The present study was designed to test the hypothesis that NRF2 contributes to pulmonary protection against hyperoxic injury in mice. Mice with site-directed mutation (knockout) of *Nrf2* (*Nrf2*$^{-/-}$) and *wt* mice (*Nrf2*$^{+/+}$) were exposed to hyperoxia, and pulmonary permeability, inflammatory, and epithelial injury responses in bronchoalveolar lavage fluid (BALF) were compared in both genotypes of mice. The effects of hyperoxia exposure on lung NRF2 mRNA expression and DNA-binding activity in *wt* mice were determined by Northern blot analysis and electrophoretic mobility shift analysis (EMSA), respectively. Lung mRNA expression for selected ARE-responsive defense enzymes were examined in *Nrf2*$^{-/-}$ and *wt* mice to identify molecular mechanisms through which NRF2 may contribute to the protection against oxidative lung injury.

Materials and Methods

Animals

Breeding pairs of ICR/Sv129-*Nrf2*$^{+/-}$ mice were obtained from a colony at Tsukuba University (17) and maintained in the Johns Hopkins facility. Mice were fed a purified AIN-76A diet. Water was provided *ad libitum*. Mice were bred, and progeny were genotyped for *Nrf2*$^{+/+}$ and *Nrf2*$^{-/-}$ (17). Cages were placed in laminar flow hoods with high-efficiency particulate-filtered air. Sentinel animals were examined periodically (titers and necropsy) for infection. All experimental protocols conducted in the mice were performed in accordance with the standards established by the US Animal Welfare Acts, set forth in NIH guidelines and the Policy and Procedures Manual (Johns Hopkins University School of Hygiene and Public Health Animal Care and Use Committee).

Oxygen Exposure

Mice were placed on a fine mesh wire flooring in a sealed 45-liter glass exposure chamber. The chamber bottom was lined with CO_2 absorbent (Soda-sorb; WR Grace, Lexington, MA). Food and water were provided *ad libitum*. Sufficient humidified pure oxygen was delivered to the chamber to provide 10 changes/h (7 liters/min flow rate). The concentration of oxygen in the exhaust from the chamber was monitored (OM-11; Beckman, Irvine, CA) throughout the experiments. The oxygen concentration for all experiments ranged from 95–99%. The chambers were opened once a day for 10 min to replace CO_2 absorbent, food, and water. Age- and gender-matched (6- to 8-wk) mice of each genotype (*Nrf2*$^{+/+}$ and *Nrf2*$^{-/-}$) were exposed to either room air or hyperoxia for 48 and 72 h (n = 4 per group).

BALF and Phenotyping

Immediately following exposure, mice were removed from the chamber, anesthetized with sodium pentobarbital (104 mg/kg), and weighed. Hyperoxia-induced changes in lungs were assessed by total protein concentration and total and differential cell counts in BALF following procedures described previously (24). Briefly, the right lung of each mouse was lavaged *in situ* four times with Hanks' balanced salt solution (HBSS, 17.5 ml/kg, pH 7.2–7.4), and the recovered BALF was immediately cooled to 4°C. For each mouse, the four BALF returns were centrifuged (500 × g at 4°C), and the supernatant from the first BALF return was decanted for determination of total protein (an indicator of lung permeability). Protein concentration was measured following the method of Bradford as indicated in the manufacturer's procedure (Bio-Rad, Hercules, CA). The cell pellets from all lavage returns were combined and resuspended in 1 ml of HBSS. The numbers of cells (per ml total BALF return) were counted with a hemocytometer as indicators of lung injury and inflammation. An aliquot (200 μl) of BALF cell suspension was cytocentrifuged (Shandon Southern Products, Pittsburgh, PA) and stained with Wright-Giemsa stain (Diff-Quik; Baxter Scientific Products, McGaw Park, IL) for differential cell analysis. Differential counts for epithelial cells, macrophages, and PMNs were done by identifying 300 cells according to standard cytologic techniques (25). Epithelial cells in particular were identified by the presence of cilia.

Total Lung RNA Isolation and Northern Blot Analysis for NRF2 mRNA Expression

Total RNA was isolated from nonlavaged lung homogenate of each mouse according to the method of Chomczynski and Sacchi (26) as indicated in the Trizol (Life Technologies, Gaithersburg, MD) reagent specifications. Pooled total RNA from each group (15 μg) was separated on a 1.2% formaldehyde-agarose gel in 1× MOPS acid buffer and transferred overnight to a nylon membrane (Nytran; Schleicher and Schuell, Keene, NH). The membrane was UV-crosslinked, and the blot was hybridized with a double-stranded [γ^{32}P]dCTP-labeled NRF2 cDNA probe (1.8 kb) in the Perfect Hybridization Buffer (Sigma, St. Louis, MO) and evaluated autoradiographically. As a control for loading of total RNA, 18S RNA on the gel was examined by staining with ethidium bromide. The intensity of each NRF2 band was quantitated using a Gel Doc 2000 System (Bio-Rad) and normalized by the intensity of the corresponding 18S RNA band.

Lung Nuclear Protein Extraction and EMSA for NRF2 Activity

Nuclear protein extracts were prepared from pooled lung tissues of four mice in each group as previously described (27). An aliquot of 2 μg nuclear proteins was incubated on ice with a binding buffer (10 mM HEPES [pH 7.9], 60 mM KCl, 0.5 mM EDTA, 4% Ficoll, 1 mM DTT, 0.2 μg PolydI-dC, 1 mM PMSF) in a total volume of 19 μl. After 15 min incubation, 1 μl (2 × 10^4 cpm) of [γ^{32}P]dATP end-labeled double-stranded oligonucleotide containing a NF-E2-consensus sequence (5′-TGG GGA ACC TGT GCT GAG TCA CTG GAG-3′) or ARE-consensus sequence (5′-AGT CAC AGT GAC TCA GCA GAA TCT-3′) was added to the reaction and followed by an additional 30-min incubation at room temperature. The mixture was subjected to electrophoresis on a 4% polyacrylamide gel with 0.25× TBE buffer for 2 h at 180 V. The gel was autoradiographed using an intensifying screen at −70°C. The intensity of each shifted band was quantitated using a Gel Doc 2000 System (Bio-Rad).

RT-PCR for Lung Antioxidant Enzyme mRNA Expression

Total RNA (500 ng) was reverse transcribed into cDNA in a volume of 50 μl, containing 1× PCR buffer (50 mM KCl and 10 mM Tris [pH 8.3]), 5 mM $MgCl_2$, 1 mM each dNTPs, 125 ng oligo $(dT)_{15}$, and 50 U of Moloney Murine Leukemia Virus reverse transcriptase (Life Technologies), at 45°C for 15 min and 95°C for 5 min using gene amp PCR System 9700 (Perkin Elmer Applied Biosystems, Foster City, CA). Separate but simultaneous PCR amplifications were performed with aliquots of cDNA (10 μl) at a final concentration of 1× PCR buffer, 4 mM $MgCl_2$, 400 μM

dNTPs, and 1.25 U *Taq* Polymerase (Life Technologies) in a total volume of 12.5 μl using 240 nM each of forward and reverse primers (Table 1) specific for mouse GST-Ya, -Yc, and -Yp_1 and rat GST-Yb_1; mouse NQO1; UDP glycosyl transferase (UGT); GCLS; HO-1; GPx1 and 2; GR; SODs 1, 2, and 3; and catalase. β-actin was used as an internal control. PCR was started with 5 min incubation at 94°C followed by a three-step temperature cycle: denaturation at 94°C for 30 s, annealing at 55–60°C for 30 s, and extension at 72°C for 1 to ~2 min for 25 to ~30 cycles (*see* Table 1). A final extension step at 72°C for 10 min was included after the final cycle to complete polymerization. The number of cycles was chosen to ensure that amplification product did not reach a plateau level. Reactions were electrophoresed in 2% agarose gel containing ethidium bromide. The volume of each cDNA band was quantitated using a Gel Doc 2000 System (Bio-Rad), and the ratio of each gene cDNA to β-actin cDNA was determined.

Lung Cytosol Preparation

For preparation of crude cytosol, right lung tissues from four mice of each group were pooled and homogenized in ice-cold 10 mM Tris-HCl (pH 7.8). The homogenates were centrifuged at 10,000 × *g* for 20 min at 4°C. Protein concentration of the resulting supernatant was determined using the Bradford assay (Bio-Rad). Aliquots of the supernatant were stored at −70°C.

Lung NQO1 Assay

Dicoumarol-sensitive NQO1 activity was measured in cytosolic fractions at 25°C by a method reported by Shaw and colleagues (28). The reaction mixture contained 30 μg cytosolic protein, 25 mM Tris-HCl (pH 7.4), 0.23 mg/ml crystalline bovine serum albumin, 0.01% (vol/vol) polyethylene sorbitan monolaurate (Tween 20, Bio-Rad), 5 μM FAD, 0.2 mM NADH, and 0 or 10 μM dicoumarol in a final volume of 200 μl. To initiate the reaction, 40 μM of 2,6-dichloroindophenol (electron acceptor) was added, and the initial velocity of the reduction of dichloroindophenol was measured spectrophotometrically at 600 nm ($a_M = 2.1 \times 10^4$ M/cm). The nonenzymatic rate measured in the presence of dicoumarol was subtracted from the uninhibited rate (i.e., rate in the absence of dicoumarol). Activity was measured three times, and group mean activity was expressed as nmol/min/mg protein.

Lung Total GST Assay

Total GST activity of the cytosolic preparation was measured spectrophotometrically at 25°C according to procedures published previously (29). Cytosolic protein (45 μg) was added to a 200-μl reaction mixture containing 100 mM KH_2PO_4 (pH 6.5) and 1 mM glutathione. Formation of the thioether between glutathione and CDNB was monitored at 340 nm ($a_M = 9.6 \times$ mM/cm) by adding 1 mM CDNB to the reaction. Measurements were performed three times, and activity was expressed as nmol/min/mg protein.

Statistics

Data were expressed as the group mean ± standard error of the mean (SEM). Three-way analysis of variance was used to evaluate the effects of hyperoxia exposure on BALF protein and cells as well as lung antioxidant enzyme mRNA expression and activity between *Nrf2* knockout ($Nrf2^{-/-}$) and *wt* ($Nrf2^{+/+}$) mice ($n = 4$ per group). The factors in the analysis were exposure (hyperoxia or air), genotype ($Nrf2^{-/-}$ or $Nrf2^{+/+}$), and exposure time (48 or 72 h). Data sets were tested for homoscedasticity as required for parametric analyses, and data that did not meet this requirement (that is, heteroscedastic) were natural log transformed. The Student–Newman–Keuls test was used for *a posteriori* comparisons of means. All analyses were performed using a commercial statistical analysis package (SigmaStat; Jandel Scientific Software, San Rafael, CA). Statistical significance was accepted at $P < 0.05$.

Results

Effects of Targeted Disruption of *Nrf2* on Hyperoxia-Induced Lung Injury

The role of NRF2 in hyperoxic lung injury was evaluated by comparing pulmonary responses to hyperoxia in $Nrf2^{-/-}$ and $Nrf2^{+/+}$ mice. Statistically significant ($P < 0.05$) effects of genotype and time were detected on total protein and numbers of macrophages and epithelial cells recovered by BALF. No statistically significant effects of genotype, exposure, or time were found for BALF lymphocytes or PMNs. Compared with genotype-matched air controls, hyperoxia induced statistically significant increases in mean total protein concentration and numbers of BALF macrophages and epithelial cells in $Nrf2^{+/+}$ and $Nrf2^{-/-}$ mice at 72 h (Figure 1). However, the mean numbers of BALF macrophages and epithelial cells were 47 and 43% greater, respectively, in $Nrf2^{-/-}$ mice compared with those in $Nrf2^{+/+}$ mice after 72 h of hyperoxia (Figure 1). Furthermore, total protein concentration was significantly higher in $Nrf2^{-/-}$ mice compared with $Nrf2^{+/+}$ after 48 (7.6-fold) and 72 h (3.8-fold) exposure (Figure 1). The results therefore indicate that disruption of *Nrf2* significantly enhanced pulmonary sensitivity and responsivity to hyperoxic challenge.

Effect of Hyperoxia on Lung NRF2 mRNA Expression and DNA Binding Activity

Expression levels of NRF2 mRNA were measured by Northern blot analysis to determine whether hyperoxia exposure modulates mRNA levels of NRF2. NRF2 mRNA was not detectable in the lungs of air- or hyperoxia-exposed knockout mice (Figure 2A). In contrast, constitutive expression of NRF2 mRNA (2.38 Kb) was detected in the lungs of $Nrf2^{+/+}$ mice, and hyperoxia enhanced the steady-state level of NRF2 mRNA in the *wt* mice at 48 and 72 h (2- and 2.6-fold, respectively) compared with those in the air-exposed *wt* mice (Figure 2A).

NF-E2– and ARE-binding abilities of lung nuclear proteins were assessed by EMSA to determine whether hyperoxia enhances functional NRF2 activity of $Nrf2^{+/+}$ mice. The nuclear protein-DNA complex formation in the lung identified by shifted bands was greater in the mice exposed to 48 (2-fold) and 72 (3-fold) h of hyperoxia than in the air-exposed mice, regardless of DNA probe used (Figure 2B). Negligible protein binding to the DNA sequences was detected in the lungs of all $Nrf2^{-/-}$ mice (data not shown). To detect specific binding of NRF2 to these DNA sequences, we performed supershift analysis using the only commercially available anti-mouse NRF2 antibody (SC-722x; Santa Cruz Biotechnology, Santa Cruz, CA). However, we failed to obtain satisfactory supershifted bands representing antibody-NRF2-DNA complex in the lung of these mice, though the same antibody has yielded successful results when applied to liver tissue (42).

Differential Expression of Lung Antioxidant Defense Enzyme mRNAs between $Nrf2^{+/+}$ and $Nrf2^{-/-}$ Mice

Expression levels of mRNA for selected antioxidant enzymes, phase 2 detoxifying enzymes, and HO-1 were compared between $Nrf2^{+/+}$ and $Nrf2^{-/-}$ mice to identify downstream genes transcriptionally activated by NRF2 (Figure

TABLE 1
Primer sequences for RT-PCR

cDNAs		Primer sequences	Amplified size (bp)	Annealing temp (°C)	PCR cycle no.
NQO1	Forward	ATT GTA CTG GCC CAT TCA GA	1,164	60	30
	Reverse	GGC CAT TGT TTA CTT TGA GC			
GST-Ya	Forward	AAG CCA GGA CTC TCA CTA	408	55	28
	Reverse	AAG GCA GTC TTG GCT TCT			
GST-Yb_1	Forward	AAG ACC ACA GCA CCA GCA CCA T	301	55	30
	Reverse	CTC TCC TCC TCT GTC TCT CCA T			
GST-Yc	Forward	GGA AGC CAG TCC TTC ATT ACT	621	55	28
	Reverse	CGT CAT CAA AAG GCT TCC TCT			
GST-Yp_1	Forward	ATG CTG CTG GCT GAC CAG GGC	576	60	25
	Reverse	ATC TTG GGC CGG GCA CTG AGG			
UGT1a6	Forward	TGA TGC TCT GTT CAC AGA CC	669	55	25
	Reverse	AAT GCC CGA GTC TTT GGA TG			
GCLS	Forward	AGG AGC TTC GGG ACT GTA TT	598	55	25
	Reverse	TGG GCT TCA ATG TCA GGG AT			
HO-1	Forward	GAG CAG AAC CAG CCT GAA CTA	200	55	25
	Reverse	GGT ACA AGG AAG CCA TCA CCA			
SOD1	Forward	ATC CAC TTC GAG CAG AAG	340	55	30
	Reverse	TTC CAC CTT TGC CCA AGT			
SOD2	Forward	AGC GGT CGT GTA AAC CTC A	439	55	30
	Reverse	AGA CAT GGC TGT CAG CTT C			
SOD3	Forward	GGT GCA GAG AAC CTC AGC C	518	55	30
	Reverse	TGC GCA CCA CGA AGT TGC C			
GPx1	Forward	AGT ACG GAT TCC ACG TTT GA	533	55	35
	Reverse	GGA ACT TCT CAA AGT TCC AG			
GPx2	Forward	GAC TTC AAT ACG TTC AGA GG	390	55	35
	Reverse	GGA ACT TCT CAA AGT TCC AG			
GR	Forward	CTT CCT TCG ACT ACC TGG	400	55	35
	Reverse	ATG CCT GCG ATC TCC ACA			
Catalase	Forward	AAT CCT ACA CCA TGT CGG ACA	726	55	28
	Reverse	CGG TCT TGT AAT GGA ACT TGC			
β-Actin	Forward	GTG GGC CGC TCT AGG CAC CA	341	57	25
	Reverse	CGG TTG GCC TTA GGG TTC AGG			

3). β-Actin mRNA expression was not significantly different between genotypes or exposures (data not shown). Hyperoxia significantly increased the mRNA expression for NQO1 (48 and 72 h), GST-Ya (72 h), UGT (72 h), GPx2 (48 and 72 h), and HO-1 (48 and 72 h) in the $Nrf2^{+/+}$ mice over basal levels (Figure 3). The induced gene levels of all these enzymes as well as basal mRNA levels of NQO1 and UGT in the $Nrf2^{+/+}$ mice were significantly higher than those in the $Nrf2^{-/-}$ animals, although UGT and HO-1mRNAs were also inducible in the $Nrf2^{-/-}$ mice after hyperoxia (Figure 3). The steady-state expression level of GST-Yc mRNA was upregulated by hyperoxia exposure in the $Nrf2^{-/-}$ mice but not in the *wt* mice. However, both baseline and induced mRNA levels of GST-Yc in the *wt* mice were significantly greater than those in similarly exposed $Nrf2^{-/-}$ mice (Figure 3). Northern blot analyses were used to confirm small, but statistically significant, differences in enzyme gene expression as detected by reverse transcriptase polymerase chain reaction (RT-PCR) (data not shown).

The differential mRNA expression of all antioxidant defense enzymes assessed between $Nrf2^{+/+}$ and $Nrf2^{-/-}$ mice

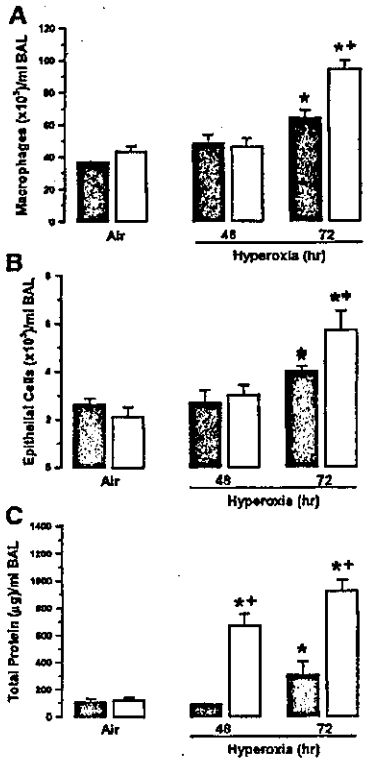

Figure 1. Effect of targeted gene disruption (knockout) of *Nrf2* on hyperoxia-induced changes in lung macrophages (*A*), epithelial cells (*B*), and total protein (*C*). Data are presented as means ± SEM ($n = 4$ per group). *Significantly different from genotype-matched air-control mice ($P < 0.05$). +Significantly greater than time-matched $Nrf2^{+/+}$ mice ($P < 0.05$). *Solid bars*, $Nrf2^{+/+}$; *open bars*, $Nrf2^{-/-}$.

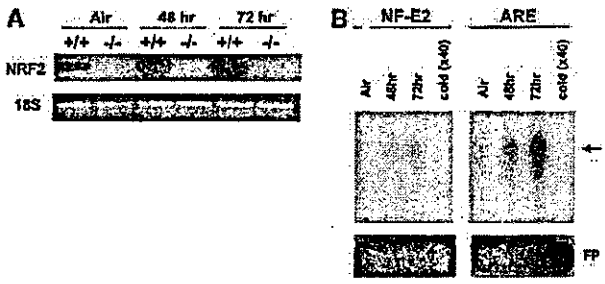

Figure 2. (*A*) The expression of NRF2 mRNA in the lungs of $Nrf2^{+/+}$ and $Nrf2^{-/-}$ mice after 48 and 72 h exposure to either air or hyperoxia. Aliquots of total-lung RNA isolated from each mouse were pooled for each group ($n = 4$ mice/group), and 2.38-kb NRF2 mRNA was detected by Northern blot analysis. (*B*) EMSA of lung nuclear proteins for NF-E2- and ARE-binding activity in $Nrf2^{+/+}$ mice exposed to either air or hyperoxia (48 and 72 h). Nuclear protein extracts from pooled lung homogenates (2 μg) of mice exposed to room air or hyperoxia ($n = 4$ mice per group) were incubated with an end-labeled oligonucleotide probe containing an NF-E2 or ARE consensus sequence. A reaction mixture was also incubated with 40-fold excess amount of each unlabeled probe to determine the specificity of NF-E2 or ARE binding proteins in the nuclear extracts, which resulted in an elimination of the protein-DNA binding activities (cold lane). *Arrow* indicates shifted bands (NF-E2– or ARE-protein complex). FP indicates free probes.

exposed to either hyperoxia or air are summarized in Figure 4. In addition to those discussed above, the steady-state levels of mRNAs for GCLS (48 and 72 h), GPx1 (72 h), and GR (72 h) were markedly enhanced in the $Nrf2^{+/+}$ mice by hyperoxia, whereas the mRNA level for SOD2 (48 and 72 h) was significantly elevated only in the $Nrf2^{-/-}$ mice (*see* Figure 4). However, no significant differences in the abundance of these enzyme mRNAs were detected between $Nrf2^{+/+}$ and $Nrf2^{-/-}$ mice. No statistically significant effects of either hyperoxia or genotype were found on the mRNA levels of GST-Yb_1 and SODs 1 and 3 (*see* Figure 4).

Differential Activities of Lung Phase 2 Enzymes Between $Nrf2^{+/+}$ and $Nrf2^{-/-}$ Mice

Basal NQO1 activity was 50% greater in the lungs of $Nrf2^{+/+}$ mice compared with $Nrf2^{-/-}$ mice (Figure 5A). Hyperoxia significantly enhanced NQO1 activity in lung cytosol of $Nrf2^{+/+}$ mice at 48 and 72 h (55 and 74%, respectively). Hyperoxia did not change lung NQO1 activity in $Nrf2^{-/-}$ mice. Furthermore, NQO1 activity in hyperoxia-exposed $Nrf2^{-/-}$ mice was significantly lower than that in similarly exposed $Nrf2^{+/+}$ mice.

The total GST activity measured in *wt* mice exposed to either air or hyperoxia (72 h) was significantly higher (1.6- to ~ 2.2-fold) than that measured in the corresponding $Nrf2^{-/-}$ mice (Figure 5B). No exposure-induced changes were observed in the total GST activity in the lungs of both genotypes of mice.

Discussion

We have demonstrated that NRF2 contributes to the protection against hyperoxic lung injury in mice. Compared with *wt* mice, mice lacking NRF2 expression and activity had significantly enhanced lung damage characterized by increased protein permeability, macrophage inflammation, and epithelial injury after hyperoxia exposure. Upregulation of NRF2 mRNA and increased DNA binding of nuclear NRF2 was found in the lungs of *wt* mice in response to hyperoxia. Furthermore, significant attenuation in basal and/or hyperoxia-induced mRNA expression of NQO1, GST-Ya and -Yc (which compose the class α GST in rodents), UGT, HO-1, and GPx2 was observed in the lungs of mice deficient in *Nrf2*, relative to the *wt* mice. This suggests that these enzyme genes are downstream effector molecules transcriptionally activated by NRF2 in the lungs of mice. NRF2-mediated pulmonary protection against hyperoxia may be attributed at least in part to these enzymes.

Previous studies using *Nrf2*-knockout mice and *Nrf2*-transfected or -deficient cell lines demonstrated that NRF2, in association with other transcription factors such as c-Jun and small Maf, plays an essential role in preventing carcinogenesis of cells or tissues (e.g., liver) (17, 21, 30, 31). This activity is thought to occur via ARE-mediated induction of phase 2 detoxifying enzymes including NQO1, GST, or GCLS. Chan and Kan have suggested a protective role of NRF2 against butylated hydroxytoluene (BHT) through the

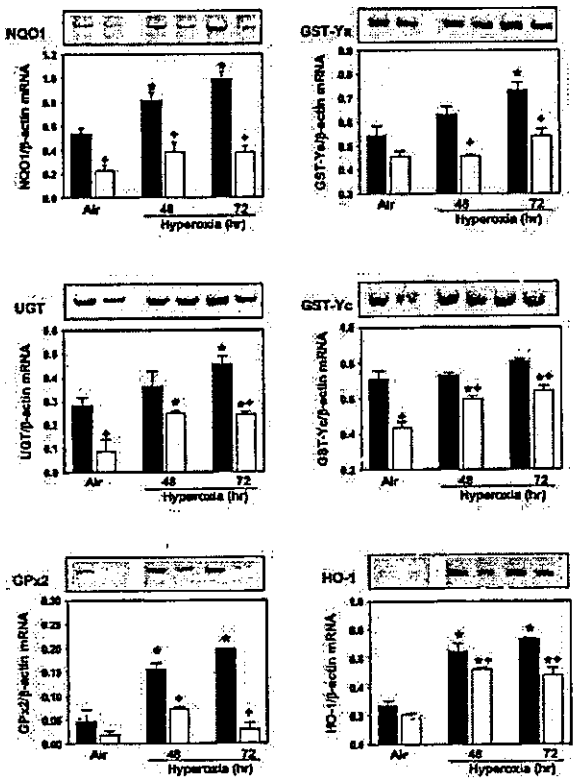

Figure 3. Differential expression of antioxidant defense enzymes in the lungs of $Nrf2^{+/+}$ and $Nrf2^{-/-}$ mice exposed to either air or hyperoxia (48 and 72 h). Total-lung RNA was isolated from each mouse, and each enzyme cDNA was amplified by RT-PCR using specific primers as indicated in Table 1 and separated on ethidium bromide-stained 1.2 to ~ 2% agarose gel. Digitized images of cDNA bands from each mouse were quantitated using a Gel Doc Analysis System and normalized to β-actin cDNA (an internal control). All data are presented as the group means ± SEM (n = 4 mice per group). Representative agarose gel images for each enzyme are shown on top of the graphs, and the order of individual cDNA bands corresponds to that of graph bars. *Significantly different from genotype-matched air-control mice ($P < 0.05$). +Significantly different from exposure and time-matched $Nrf2^{+/+}$ mice ($P < 0.05$). *Solid bars*, $Nrf2^{+/+}$; *open bars*, $Nrf2^{-/-}$.

activation of pulmonary antioxidant defense enzymes (19). These investigators demonstrated that *Nrf2*-knockout mice exposed to BHT had more severe acute lung injury and lower levels of lung mRNA transcripts for antioxidant defense enzymes including NQO1, UGT, catalase, and SOD1 than similarly exposed *wt* mice. The potential contribution of NRF2 in oxidative tissue injury has been demonstrated in a study by Ishii and colleagues (22), who reported that peritoneal macrophages isolated from electrophile-susceptible *Nrf2*-knockout mice had impaired mRNA induction of HO-1, A170, and peroxiredoxin MSP23. They concluded that NRF2 is a key transcription factor for oxidative stress-inducible proteins. The present study, to our knowledge, is the first to demonstrate a protective role of NRF2 in oxidative tissue injury of the lungs.

We have determined that both basal and hyperoxia-inducible NQO1 expression are NRF2 dependent in the murine lungs. In addition, transcriptional regulation of GST isozyme α and UGT was also at least in part mediated through NRF2 in this model. Consistent with their NRF2-dependent gene expression patterns, enzyme activities for lung NQO1 were significantly higher in *wt* mice than in $Nrf2^{-/-}$ mice. Total GST activity, which is attributed to all isoenzymes (e.g., α, μ, π, and θ), was also significantly higher in *wt* mice than in $Nrf2^{-/-}$ mice following air or hyperoxia exposure. Although the total GST activity does not discriminate between the contributions of the various isoenzymes, results largely reflected the mRNA expression pattern of α GST (composed of Ya and Yc subunits; *see* Figure 3). The antioxidant role of phase 2 detoxifying enzymes has been widely examined in cells and several tissues due to their protection against toxic and neoplastic effects of electrophilic metabolites or ROS generated by chemical carcinogenes or xenobiotics (14, 15). Moreover, as a component of the glutathione redox system, GST has been postulated to provide protection to the lung from oxidative injury induced by toxicants (32). However, only one previous study has investigated the contribution of phase 2 enzymes to the hyperoxic lung injury in laboratory animals (33). In that study, increased pulmonary NQO1 activity by pretreatment with 3-methylcholanthrene and BHT did not significantly improve the survival rate of rats exposed to hyperoxia. Our observations suggest that in addition to conjugating reactive electrophilis or xenobiotics, phase 2 detoxifying enzymes may also exert indirect antioxidant functions in the hyperoxic lungs of mice. However, functional analyses are necessary to establish their importance in the pathogenesis of oxidative lung injury.

Accumulating evidence has suggested that the microsomal enzyme HO-1 is highly inducible as a protective mechanism by various oxidative stresses, including hyperoxia (13, 34) and electrophiles that induce phase 2 enzymes (35). Recent *in vitro* studies (20, 36) and an *in vivo* study using *Nrf2* gene-knockout mice (22) have determined that NRF2 upregulates ARE-mediated HO-1 expression. The present study demonstrated that hyperoxia-inducible lung HO-1 expression is partially mediated through NRF2. Interestingly, we also observed a significant induction of HO-1 mRNA in the $Nrf2^{-/-}$ mice by hyperoxia challenge, which could be explained by evidence indicating that either NF-κB (37) or AP-1 (38) plays a role in the transcriptional regulation of HO-1.

Among lung classical antioxidant enzymes, regulation of mRNA for GPx2, a recently identified isoform of cellular GPxs in the gastrointestine of rodents (39), was largely NRF2-dependent in the lungs of hyperoxia-exposed mice. To date, only GPx1 has been widely investigated as the representative isoform of cellular GPx in the lungs of laboratory animals. However, a study using a mouse model with targeted disruption of GPx1 demonstrated that the hyperoxic survival rate was not increased in GPx1-deficient mice (40). The results from this and our current study suggest an important role of GPx2 as a critical component of pulmonary antioxidant defense system. We found that catalase and SOD (1, 2, and 3) mRNA expression were not dependent on NRF2 in the hyperoxic lungs. It is likely

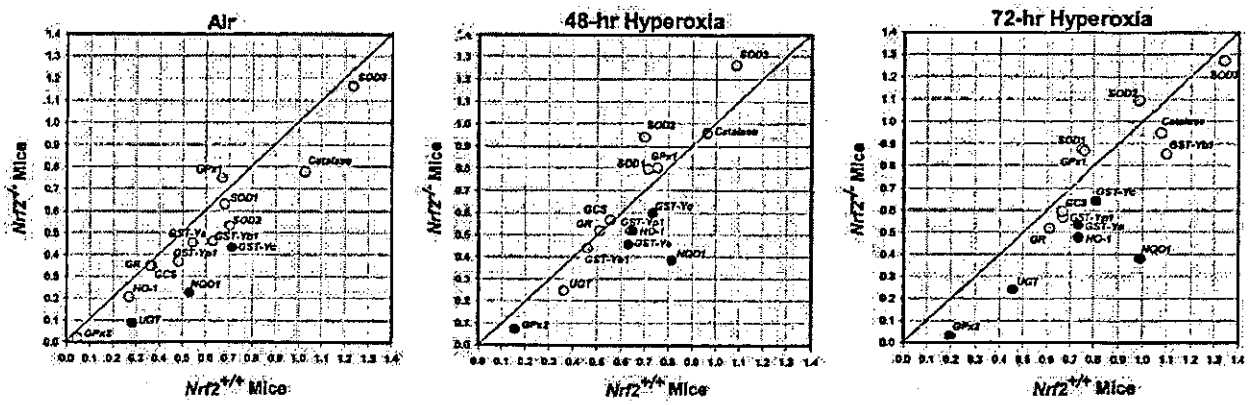

Figure 4. Ratio of mean ($n = 4$ per group) mRNA levels for lung antioxidant defense enzymes determined by semi-quantitative RT-PCR to elucidate genotype ($Nrf2^{+/+}$, $Nrf2^{-/-}$) effects on each enzyme gene expression after air or hyperoxia (48 and 72 h) exposure. *Black circles* show enzymes of which mRNA levels vary significantly between two genotypes, and *gray circles* show others.

that the contribution of NRF2 to the induction of these lung antioxidant enzymes may be very limited in the protection against oxygen toxicity. These observations are inconsistent with the results from a previous study in which BHT treatment induced mRNA expression of SOD1 and catalase via NRF2 (19).

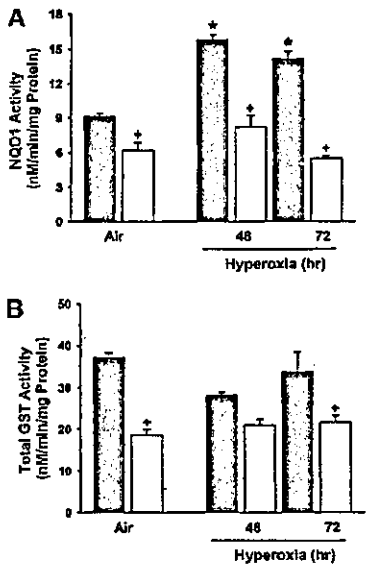

Figure 5. Differential enzyme activity of NQO1 and total GST in the lungs of $Nrf2^{+/+}$ and $Nrf2^{-/-}$ mice exposed to either air or hyperoxia (48 and 72 h). Cytosolic protein was prepared from pooled lung homogenates of each group. Enzymatic activity of NQO1 in 30-μg protein was measured spectrophotometrically using 2,6-dichloroindophenol as the electron acceptor in the presence or absence of dicoumarol (*A*). Enzymatic activity of total GST in 45-μg protein was measured spectrophotometrically using CDNB as the enzyme substrate (*B*). Data are presented as the group means ± SEM from three separate measurements. *Significantly higher than genotype-matched air-control mice ($P < 0.05$). +Significantly lower than exposure and time-matched $Nrf2^{+/+}$ mice ($P < 0.05$). *Solid bars*, $Nrf2^{+/+}$; *open bars*, $Nrf2^{-/-}$.

The present study also demonstrates that hyperoxia exposure enhances expression of NRF2 mRNA and functionally activated nuclear NRF2 in the lungs of normal (*wt*) mice. The regulatory mechanisms of NRF2 have been largely unknown with the exception of Keap1, a cytoplasmic chaperone that suppresses NRF2 transcriptional activity by specific binding to the N-terminal regulatory domain (Neh2) of NRF2 (41). Ishii and colleagues (22) postulated that NRF2 may be activated at the posttranslation level, probably by deactivation of Keap1 and, in turn, induction of NRF2 nuclear translocation. However, upregulation of the liver NRF2 mRNA level and a subsequent increase of nuclear NRF2 translocation has been reported in a recent *in vivo* study with mice treated with a cancer chemoprotective agent (42). This recent investigation and our present observation provide new understanding of the regulatory mechanisms of NRF2.

In conclusion, we determined that NRF2 plays a significant role in the protection against hyperoxic pulmonary injury in mice possibly by transcriptional activation of lung antioxidant defense enzymes. The results from our study add a potential protective mechanism through NRF2 and a putative role of phase 2 detoxifying enzymes as indirect antioxidants in oxidative lung injury.

Acknowledgments: The authors acknowledge the contribution of the Johns Hopkins University NIEHS Center-supported Inhalation Facility to this project. This work was supported by National Institutes of Health grants ES-03819, ES-09606, HL-58122, HL-66109, HL-57142, and CA-44530 and by Environmental Protection Agency grant R-825815.

References

1. Halliwell, B., J. M. Gutteridge, and C. E. Cross. 1992. Free radicals, antioxidants, and human disease: where are we now? *J. Lab. Clin. Med.* 119:598–620.
2. Crapo, J. D., B. E. Barry, H. A. Foscue, and J. Shelburne. 1980. Structural and biochemical changes in rat lungs occurring during exposure to lethal and adaptive doses of oxygen. *Am. Rev. Respir. Dis.* 122:123–143.
3. Crapo, J. D. 1986. Morphologic changes in pulmonary oxygen toxicity. *Ann. Rev. Physiol.* 48:721–731.
4. Clerch, L. B., and D. J. Massaro. 1993. Tolerance of rats to hyperoxia. *J. Clin. Invest.* 91:499–508.
5. Clark, J. M., and C. J. Lambertsen. 1971. Pulmonary oxygen toxicity: a review. *Pharmacol. Rev.* 23:37–133.
6. Ho, Y. S., M. S. Dey, and J. D. Crapo. 1996. Antioxidant enzyme expression in rat lungs during hyperoxia. *Am. J. Physiol.* 270(5, Pt. 1):L810–L818.

7. Clerch, L. B. 2000. Post-transcriptional regulation of lung antioxidant enzyme gene expression. *Ann. NY Acad. Sci.* 899:103–111.
8. Folz, R. J., A. M. Abushamaa, and H. B. Suliman. 1999. Extracellular superoxide dismutase in the airways of transgenic mice reduces inflammation and attenuates lung toxicity following hyperoxia. *J. Clin. Invest.* 103:1055–1066.
9. Ho, Y. S., R. Vincent, M. S. Dey, J. W. Slot, and J. D. Crapo. 1998. Transgenic models for the study of lung antioxidant defense: enhanced manganese-containing superoxide dismutase activity gives partial protection to B6C3 hybrid mice exposed to hyperoxia. *Am. J. Respir. Cell Mol. Biol.* 18: 538–547.
10. Tsan, M. F., J. E. White, B. Caska, C. J. Epstein, and C. Y. Lee. 1998. Susceptibility of heterozygous MnSOD gene-knockout mice to oxygen toxicity. *Am. J. Respir. Cell Mol. Biol.* 19:114–120.
11. Danel, C., S. C. Erzurum, P. Prayssac, N. T. Eissa, R. G. Crystal, P. Herve, B. Baudet, M. Mazmanian, and P. Lemarchand. 1998. Gene therapy for oxidant injury-related diseases: adenovirus-mediated transfer of superoxide dismutase and catalase cDNAs protects against hyperoxia but not against ischemia-reperfusion lung injury. *Hum. Gene Ther.* 9:1487–1496.
12. Choi, A. M., and J. Alam. 1996. Heme oxygenase-1: function, regulation, and implication of a novel stress-inducible protein in oxidant-induced lung injury. *Am. J. Respir. Cell Mol. Biol.* 15:9–19.
13. Otterbein, L. E., J. K. Kolls, L. L. Mantell, J. L. Cook, J. Alam, and A. M. Choi. 1999. Exogenous administration of heme oxygenase-1 by gene transfer provides protection against hyperoxia-induced lung injury. *J. Clin. Invest.* 103:1047–1054.
14. O'Brien, P. J. 1991. Molecular mechanisms of quinone cytotoxicity. *Chem. Biol. Interact.* 80:1–41.
15. Fahey J. W., and P. Talalay. 1999. Antioxidant functions of sulforaphone: a potent inducer of phase II detoxication enzymes. *Food Chem. Toxicol.* 37:973–979.
16. Chan, K., R. Lu, J. C. Chang, and Y. W. Kan. 1996. NRF2, a member of the NFE2 family of transcription factors, is not essential for murine erythropoiesis, growth, and development. *Proc. Natl. Acad. Sci. USA* 93:13943–13948.
17. Itoh, K., T. Chiba, S. Takahashi, T. Ishii, K. Igarashi, Y. Katoh, T. Oyake, N. Hayashi, K. Satoh, I. Hatayama, M. Yamamoto, and Y. Nabeshima. 1997. An Nrf2/small Maf heterodimer mediates the induction of phase II detoxifying enzyme genes through antioxidant response elements. *Biochem. Biophys. Res. Commun.* 236:313–322.
18. Hayes, J. D., S. A. Chanas, C. J. Henderson, M. McMahon, C. Sun, G. J. Moffat, C. R. Wolf, and M. Yamamoto. 2000. The Nrf2 transcription factor contributes both to the basal expression of glutathione S-transferases in mouse liver and to their induction by the chemopreventive synthetic antioxidants, butylated hydroxyanisole and ethoxyquin. *Biochem. Soc. Trans.* 28:33–41.
19. Chan, K., and Y. W. Kan. 1999. Nrf2 is essential for protection against acute pulmonary injury in mice. *Proc. Natl. Acad. Sci. USA* 96:12731–12736.
20. Alam, J., D. Stewart, C. Touchard, S. Boinapally, A. M. Choi, and J. L. Cook. 1999. Nrf2, a Cap'n'Collar transcription factor, regulates induction of the heme oxygenase-1 gene. *J. Biol. Chem.* 274:26071–26078.
21. Venugopal, R., and A. K. Jaiswal. 1998. Nrf2 and Nrf1 in association with Jun proteins regulate antioxidant response element-mediated expression and coordinated induction of genes encoding detoxifying enzymes. *Oncogene* 17:3145–3156.
22. Ishii, T., K. Itoh, S. Takahashi, H. Sato, T. Yanagawa, Y. Katoh, S. Bannai, and M. Yamamoto. 2000. Transcription factor Nrf2 coordinately regulates a group of oxidative stress-inducible genes in macrophages. *J. Biol. Chem.* 275:16023–16029.
23. Moinova, H. R., and R. T. Mulcahy. 1999. Up-regulation of the human gamma-glutamylcysteine synthetase regulatory subunit gene involves binding of Nrf-2 to an electrophile responsive element. *Biochem. Biophys. Res. Commun.* 261:661–668.
24. Kleeberger, S. R., R. C. Levitt, L. Zhang, M. Longphre, J. Harkema, A. Jedlicka, S. Eleff, D. DiSilvestre, and K. J. Holroyd. 1997. Linkage analysis of susceptibility to ozone-induced lung inflammation in inbred mice. *Nat. Genet.* 17:475–478.
25. Saltini, C., A. J. Hance, V. J. Ferrans, F. P. B. Bassett, and R. G. Crystal. 1984. Accurate quantitation of cells recovered by bronchoalveolar lavage. *Am. Rev. Respir. Dis* 130:650–658.
26. Chomczynski, P., and N. Sacchi. 1987. Single-step method of RNA isolation by acid guanidinium thiocyanate-phenol-chloroform extraction. *Anal. Biochem.* 162:156–159.
27. Lahiri, D. K., and Y. Ge. 2000. Electrophoretic mobility shift assay for the detection of specific DNA-protein complex in nuclear extracts from the cultured cells and frozen autopsy human brain tissue. *Brain Res. Brain Res. Protoc.* 5:257–265.
28. Shaw, P. M., A. Reiss, M. Adesnik, D. W. Nebert, J. Schembri, and A. K. Jaiswal. 1991. The human dioxin-inducible NAD(P)H: quinone oxidoreductase cDNA-encoded protein expressed in COS-1 cells is identical to diaphorase 4. *Eur. J. Biochem.* 195:171–176.
29. Habig, W. H., M. J. Pabst, and W. B. Jakoby. 1974. Glutathione S-transferases: the first enzymatic step in mercapturic acid formation. *J. Biol. Chem.* 249:7130–7139.
30. Venugopal, R., and A. K. Jaiswal. 1996. Nrf1 and Nrf2 positively and c-Fos and Fra1 negatively regulate the human antioxidant response element-mediated expression of NAD(P)H:quinone oxidoreductase1 gene. *Proc. Natl. Acad. Sci. USA* 93:14960–14965.
31. Jeyapaul, J., and A. K. Jaiswal. 2000. Nrf2 and c-Jun regulation of antioxidant response element (ARE)-mediated expression and induction of gamma-glutamylcystein synthetase heavy subunit gene. *Biochem. Pharmacol.* 59:433–439.
32. Rahman, Q., P. Abidi, F. Afaq, D. Schiffmann, B. T. Mossman, D. W. Kamp, and M. Athar. 1999. Glutathione redox system in oxidative lung injury. *Crit. Rev. Toxicol.* 29:543–568.
33. Whitney, P. L., and L. Frank. 1993. Does lung NAD(P)H:quinone reductase (DT-diaphorase) play an antioxidant enzyme role in protection from hyperoxia? *Biochim. Biophys. Acta* 1156:275–282.
34. Lee, P. J., J. Alam, G. W. Wiegand, and A. M. Choi. 1996. Overexpression of heme oxygenase-1 in human pulmonary epithelial cells results in cell growth arrest and increased resistance to hyperoxia. *Proc. Natl. Acad. Sci. USA* 93:10393–10398.
35. Prestera, T., P. Talalay, J. Alam, Y. I. Ahn, P. J. Lee, and A. M. Choi. 1995. Parallel induction of heme oxygenase-1 and chemoprotective phase 2 enzymes by electrophiles and antioxidants: regulation by upstream antioxidant-responsive elements (ARE). *Mol. Med.* 1:827–837.
36. Alam J., C. Wicks, D. Stewart, P. Gong, C. Touchard, S. Otterbein, A. M. Choi, M. E. Burow, and J. S. Tou. 2000. Mechanism of heme oxygenase-1 gene activation by cadmium in MCF-7 mammary epithelial cells role of p38 kinase and Nrf2 transcription factor. *J. Biol. Chem.* 275:27694–27702.
37. Kurata, S., M. Matsumoto, Y. Tsuji, and H. Nakajima. 1996. Lipopolysaccharide activates transcription of the heme oxygenase gene in mouse M1 cells through oxidative activation of nuclear factor kappa B. *Eur. J. Biochem.* 239:566–571.
38. Camhi, S. L., J. Alam, G. W. Wiegand, B. Y. Chin, and A. M. Choi. 1998. Transcriptional activation of the HO-1 gene by lipopolysaccharide is mediated by 5′ distal enhancers: role of reactive oxygen intermediates and AP-1. *Am. J. Respir. Cell Mol. Biol.* 18:226–234.
39. Brigelius-Flohe, R. 1999. Tissue-specific functions of individual glutathione peroxidases. *Free Radic. Biol. Med.* 27:951–965.
40. Ho, Y. S., J. L. Magnenat, R. T. Bronson, J. Cao, M. Gargano, M. Sugawara, and C. D. Funk. 1997. Mice deficient in cellular glutathione peroxidase develop normally and show no increased sensitivity to hyperoxia. *J. Biol. Chem.* 272:16644–16651.
41. Itoh, K., N. Wakabayashi, Y. Katoh, T. Ishii, K. Igarashi, J. D. Engel, and M. Yamamoto. 1999. Keap1 represses nuclear activation of antioxidant responsive elements by Nrf2 through binding to the amino-terminal Neh2 domain. *Genes Dev.* 13:76–86.
42. Kwak, M. K., K. Itoh, M. Yamamoto, T. R. Sutter, and T. W. Kensler. 2001. Role of transcriptional factor Nrf2 in the induction of hepatic phase 2 and antioxidant enzymes *in vivo* by the cancer chemoprotective agent, 3H-1,2-dithiole-3-thione. *Mol. Med.* 7:135–145.

MOLECULAR AND CELLULAR BIOLOGY, May 2002, p. 2883–2892 Vol. 22, No. 9
0270-7306/02/$04.00+0 DOI: 10.1128/MCB.22.9.2883–2892.2002

Enhanced Expression of the Transcription Factor Nrf2 by Cancer Chemopreventive Agents: Role of Antioxidant Response Element-Like Sequences in the *nrf2* Promoter

Mi-Kyoung Kwak,[1] Ken Itoh,[2] Masayuki Yamamoto,[2] and Thomas W. Kensler[1]*

Department of Environmental Health Sciences, Johns Hopkins Bloomberg School of Public Health, Baltimore, Maryland,[1] and Institute of Basic Medical Sciences and Center for Tsukuba Advanced Research Alliance, University of Tsukuba, Tennoudai, Tsukuba, Japan[2]

Received 11 September 2001/Returned for modification 16 October 2001/Accepted 24 January 2002

Induction of phase 2 enzymes, which neutralize reactive electrophiles and act as indirect antioxidants, is an important mechanism for protection against carcinogenesis. The transcription factor Nrf2, which binds to the antioxidant response element (ARE) found in the upstream regulatory region of many phase 2 genes, is essential for the induction of these enzymes. We have investigated the effect of the potent enzyme inducer and anticarcinogen 3*H*-1,2-dithiole-3-thione (D3T) on the fate of Nrf2 in murine keratinocytes. Both total and nuclear Nrf2 levels increased rapidly and persistently after treatment with D3T but could be blocked by cotreatment with cycloheximide. Nrf2 mRNA levels increased ~2-fold 6 h after D3T treatment. To examine the transcriptional activation of Nrf2 by D3T, the proximal region (1 kb) of the *nrf2* promoter was isolated. Deletion and mutagenesis analyses demonstrated that *nrf2* promoter-luciferase reporter activity was enhanced by treatment with D3T and that ARE-like sequences were required for this activation. Gel shift assays with nuclear extracts from PE cells indicated that common factors bind to typical AREs and the ARE-like sequences of the *nrf2* promoter. Direct binding of Nrf2 to its own promoter was demonstrated by chromatin immunoprecipitation assay. Overexpression of Nrf2 increased the activity of the *nrf2* promoter-luciferase reporter, while expression of mutant Nrf2 protein repressed activity. Thus, Nrf2 appears to autoregulate its own expression through an ARE-like element located in the proximal region of its promoter, leading to persistent nuclear accumulation of Nrf2 and protracted induction of phase 2 genes in response to chemopreventive agents.

Inducers of phase 2 and antioxidative enzymes are known to enhance the detoxication of environmental carcinogens in animals, often leading to protection against neoplasia (14, 24, 26). Use of enzyme inducers as cancer chemopreventive agents in humans is currently under clinical investigation (37, 41). Regulation of both basal and inducible expression of protective enzymes is mediated in part by the antioxidant response element (ARE), a *cis*-acting sequence found in the 5′-flanking region of the genes encoding many phase 2 enzymes such as mouse glutathione *S*-transferase (GST) Ya, human NAD(P)H quinone oxidoreductase (NQO1), and human γ-glutamylcysteine ligase. The core sequence of the ARE has been identified as TGACnnnGC, and several transcription factors are known to bind to the ARE (19, 28, 31, 35, 39). Among these transcription factors, members of basic leucine zipper (bZIP) NF-E2 family such as Nrf1 and Nrf2, which heterodimerize with small Maf family proteins, may be particularly important. Overexpression of Nrf1 and Nrf2 in human hepatoma cells enhanced the basal and inducible transcriptional activation of an ARE reporter gene (39). Recent studies with *nrf2*-disrupted mice indicated that Nrf2 was essential for induction of GST and NQO1 activities in vivo by many different classes of chemopreventive agents, including phenolic antioxidants, 3*H*-1,2-dithiole-3-thione (D3T), and isothiocyanates (19, 27, 30). Moreover, these knockout mice were considerably more sensitive to the toxicities of acetaminophen, butylated hydroxytoluene, and hyperoxia (4, 6, 11) and the carcinogenicity of benzopyrene (34). Collectively, these reports demonstrated a central role for Nrf2 in the regulation of basal and inducible expression of genes that defend against environmental stresses.

Nuclear levels of Nrf2 are increased when peritoneal macrophages are treated with oxidative stressors such as diethylmaleate and paraquat (18). Increased nuclear accumulation of Nrf2 has also been observed in the liver of mice treated with D3T and β-naphthoflavone (26, 27). Initially, this accumulation results from translocation of Nrf2 protein from the cytoplasm. Itoh et al. (20) have identified Keap1, a protein located in the cytoplasm that sequesters Nrf2 by specific binding to the amino-terminal regulatory domain of Nrf2. Administration of sulfhydryl reactive reagents such as diethylmaleate (which are also phase 2 inducers) abolished Keap1 repression of Nrf2 activity in cells and facilitated the nuclear accumulation of Nrf2 (20). Huang et al. (16) have recently proposed that protein kinase C-mediated phosphorylation of Nrf2 could be a critical event for the nuclear translocation of this protein. Involvement of ERK and p38 mitogen-activated protein kinase pathways in the nuclear binding of Nrf2 to the ARE have been proposed by others (45).

We have previously observed that treatment of mice with dithiolethiones led to increased steady-state mRNA levels for Nrf2 in several tissues (27, 34). In this study with a murine cell

* Corresponding author. Mailing address: Department of Environmental Health Sciences, Johns Hopkins Bloomberg School of Public Health, 615 N. Wolfe St., Baltimore, MD 21205. Phone: (410) 955-4712. Fax: (410) 955-0116. E-mail: tkensler@jhsph.edu.

culture system in which phase 2 enzymes were readily inducible, we observed that Nrf2 accumulated in nuclei and in total cellular homogenate after treatment with D3T. mRNA levels for Nrf2 were also increased after treatment. Reporter constructs containing either −35 to −1065 of the murine *nrf2* promoter or nested deletion fragments indicated that intact promoter activity was increased twofold after incubation with D3T and that this activation was blunted when the ARE-like sequences in the promoter were deleted or mutated. Overexpression of Nrf2 doubled the activity of the reporter promoter and coexpression of MafK in the cells further enhanced the promoter activity of Nrf2. However, the mutated ARE-like promoter showed no activation when Nrf2 was overexpressed. Chromatin immunoprecipitation (ChIP) with Nrf2 antibody also indicated association of Nrf2 with its promoter. Collectively, these results suggest that rapid accumulation of Nrf2 within nuclei after treatment with D3T may upregulate its own expression through ARE-like sequences in its promoter. This autoregulation of Nrf2 expression can, in turn, lead to a more sustained signaling of phase 2 gene expression.

MATERIALS AND METHODS

Reagents. All chemicals were purchased from Sigma Chemical Co. (St. Louis, Mo.), and D3T was provided by Thomas Curphey (Dartmouth Medical School, Hanover, N.H.) (10). [γ-^{32}P]ATP (4,500 Ci/mmol) was purchased from ICN (Costa Mesa, Calif.). The luciferase reporter vector pGLbasic and the assay kit were purchased from Promega (Madison, Wis.) and pTATALuc+ from the American Type Culture Collection (Manassas, Va.).

Cell culture. Murine keratinocyte PE cells were established from 12-*O*-tetradecanoyl phorbol-13-acetate (TPA)-induced murine skin papillomas as described previously (46). The cells were maintained in Eagle minimal essential medium containing 10% heat-inactivated and Chelex-treated fetal bovine serum (Life Technologies, Inc., Grand Island, N.Y.), 2 mM $CaCl_2$, and antimycotics or antibiotics (Life Technologies).

Plasmids. The sequence of the promoter region of *nrf2* (−1065 to −35) has been published (5), and this promoter was isolated by PCR amplification from hepatic genomic DNA of ICR mice. The isolated PCR product was ligated into pCR2.1 (Invitrogen, Carsbad, Calif.) and a *SacI-XhoI* fragment from this construct was recloned into the luciferase reporter vector pGLbasic (pGLNRP −1063/−35). Deleted sequences of the *nrf2* promoter (−599 to −35 and −429 to −35) were produced by PCR from the full-length promoter and ligated into pGLbasic vector (pGLNRP−599/−35, pGLNRP−429/−35). Sequences containing ARE-like 1 (−574 to −403) and ARE-like 2 (−848 to −684) were also produced by PCR and ligated into the enhancer reporter vector pTATALuc+ (pTATA AREL1, AREL2). Plasmids for overexpression of murine Nrf2 and MafK were made by ligating cDNAs generated by PCR from mouse brain cDNA (Clontech, Palo Alto, Calif.) into pcDNA3 (Promega) (5, 17). A mutant Nrf2 construct, in which the N-terminal region (amino acids 1 to 368), including the transactivation domain, was excluded, was generated as described previously (1). All plasmid sequences were confirmed by sequencing analysis by the DNA Analysis Facility of the Johns Hopkins University (Baltimore, Md.).

Site-directed mutagenesis. Mutated ARE-like sequence-containing promoters of *nrf2* were generated by site-directed mutagenesis. Primers containing mutated AREL1 (ACCGTCCTCCGCCAT) or AREL2 (GGCGTCCTGTGGCGC) were used for PCR amplification of mutated *nrf2* promoter, and PCR products were digested with *DpnI* for 1 h to cleave the wild-type promoter. The sequence of each promoter was verified.

DNA transfection and luciferase activity. Cells were transfected at 50% confluency by using Lipofectamine Plus reagent (Life Technologies). Briefly, cells were seeded in 12-well plates at a density of 3×10^4 to 4×10^4 cells/well. Cells were grown overnight, and the transfection complex containing 1 μg of plasmid DNA, 0.2 μg of pRLtk plasmid (Promega), and transfection reagent was added to each well in the absence of fetal bovine serum. Medium containing 20% fetal bovine serum was added 3 h after transfection was begun, and cells were incubated for another 16 to 18 h. Cells recovered for 6 h in normal media after removal of the transfection reagents. After incubations with inducers, cells were lysed and *Renilla* and firefly luciferase activities were measured by using the dual luciferase assay kit (Promega) with a luminometer (EG&G Wallac, Inc., Gaithersburg, Md.). Luciferase activities were normalized relative to *Renilla* luciferase activities, the internal control. For overexpression studies, pcDNA3 and pcDNA3–wild-type Nrf2, -mutant Nrf2, or -MafK constructs were cotransfected with the pGL-Nrf2 promoter. Reported luciferase activities are from three to five different transfections.

Preparation of cell extracts. Nuclear extracts from PE cells were prepared as described previously (9), and supernatant resulting from isolation of nuclei was centrifuged at 100,000 × *g* for 1 h to obtain the cytosolic fraction. Total homogenate from PE cells was prepared by disrupting cells with a glass-Teflon homogenizer in an extraction buffer containing 20 mM HEPES (pH 7.9), 1.5 mM $MgCl_2$, 420 mM NaCl, 10% glycerol, 0.2 mM EDTA, and 0.5 mM phenylmethylsulfonyl fluoride. Protein concentrations were determined by the modified Lowry method (Bio-Rad, Hercules, Calif.).

Electrophoretic mobility shift assays (EMSAs). *Nrf2* ARE-like sequence 1 (GCCCACCTGACTCCGCCATGCCC) or *Nrf2* ARE-like sequence 2 (AACT GGCGCCACAGTCAGCCGGT) was end labeled with [γ-^{32}P]ATP and incubated with 5 g of nuclear extracts from PE cells for 30 min at room temperature in a reaction mixture containing 10 mM HEPES (pH 7.9), 60 mM KCl, 0.5 mM EDTA, 4% Ficoll, 1 mM phenylmethylsulfonyl fluoride, and 0.2 g of poly(dI-dC). For competition binding, a 200-fold excess of cold AREL1 or AREL2, human *NQO1* ARE (GCAGTCACAGTGACTCAGCAGAATCT), NF-E2 (TGGGGA ACCTGTGCTGAGTCACTGGT), and AP-1 (TATCGATAAGCTATGACTC ATCCGGG) consensus binding sequences were incubated with radiolabeled AREL1 and AREL2. For immunodepletion studies, nuclear extracts from D3T-treated cells preincubated with 1 μg of Nrf2 antibody for 2 h. After incubation, loading buffer was added and the reaction products were analyzed on a 4% acrylamide gel (80:1 [acrylamide-bisacrylamide]) and exposed to X-ray film for 16 h.

SDS-PAGE and Western blotting. Total cellular homogenate (20 μg), cytosol (35 μg) and nuclear extract (12 μg) were separated by sodium dodecyl sulfate-polyacrylamide gel electrophoresis (SDS-PAGE) on a 6% polyacrylamide gel. Gels were transferred to nitrocellulose membranes (Amersham Pharmacia Biotech, Inc., Piscataway, N.J.) at 50 V for 3 h, and immunoblotting was carried out with Nrf2 antibodies reacting with the N-terminal of murine Nrf2 (27). Immunoblotted membranes were developed by using the ECL Western blotting system (Amersham Pharmacia Biotech) as described in the manufacturer's instructions.

Isolation of RNA and Northern blot hybridization. Total RNA was isolated by the procedure of Chomczynski and Sacchi (7), and RNA samples were electrophoresed on 1% agarose gels containing 2.2 M formaldehyde and then transferred to nylon membranes (Schleicher and Schuell, Keene, N.H.). cDNA for mouse Nrf2 was labeled with [γ-^{32}P]dCTP by using a random primer labeling kit (Amersham Pharmacia Biotech), hybridized, and washed as described previously (27). After being washed, the membranes were exposed to X-ray film (Eastman Kodak, Rochester, N.Y.) and developed with a Konica (Tokyo, Japan) film processor. Labeled membranes were stripped and reprobed with oligonucleotides for β-actin for loading control.

ChIP assay. Formaldehyde cross-linking and immunoprecipitations were carried out as described previously (3, 44) by using an acetyl-histone H4 ChIP assay kit (Upstate Biotechnology, Lake Placid, N.Y.). Briefly, 37% formaldehyde was directly added to cell culture medium at a final concentration of 1%. Cells were incubated for 10 min at 37°C and washed twice with ice-cold phosphate-buffered saline containing protease inhibitor cocktail (Sigma). Nuclei were isolated after Dounce homogenization and resuspended in sonication buffer (1% SDS; 10 mM EDTA; 50 mM Tris-HCl, pH 8.1; protease inhibitor cocktail). Samples were sonicated on ice to an average length of 500 to 1,000 bp by using a Sonic Dismembrator (Fisher Scientific, Pittsburgh, Pa.) and centrifuged at 12,000 rpm. The chromatin solution was diluted 10-fold with dilution buffer (0.01% SDS; 1.1% Triton X-100; 1.2 mM EDTA; 16.7 mM Tris-HCl, pH 8.1; 167 mM NaCl); one-third was reserved as a total input of chromatin. Diluted chromatin solution was precleared with salmon sperm DNA–protein A-agarose for 1 h and incubated with either anti-Nrf2 antibody, anti-GATA-1 antibody (Santa Cruz, Santa Cruz, Calif.), nonspecific immunoglobulin, or no antibody for 18 h at 4°C with rotation. Immunoprecipitation, washing, and elution were carried out according to the manufacturer's instructions. Cross-linked immunoprecipitates and total chromatin input were reversed, and samples were treated with proteinase K (Sigma) and extracted with phenol-chloroform-isoamyl alcohol (25:24:1). DNA was precipitated with ethanol and resuspended with 30 μl of water. Then, 1 μl of DNA was used for 32 to 36 cycles of PCR amplification with the following primers: *gst Ya* ARE (5′-ACTTGGCAGGAAGGATCAGT-3′ and 5′-TGCTC TAGGTCTCAGTGCAG-3′), *nrf2* AREL-2 (5′-GGCAGTTGGCCTCTTGCA AA-3′ and 5′-CCTGCAGAACCTTGCCCGCT-3′), promoter of β-*actin* (5′-C CGGTCGAGTCGC-GTCCACC-3′ and 5′-GGCGAACTGGTGGC-GGGTGT-

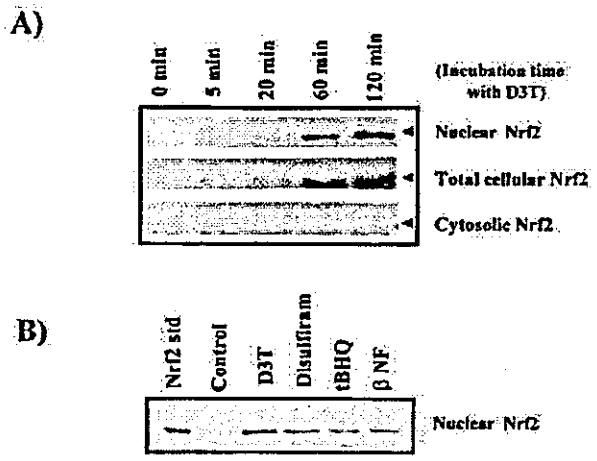

FIG. 1. Effects of D3T on levels of Nrf2 in PE cells. (A) Nrf2 levels were examined in nuclear extracts, total cellular homogenates, and cytosolic fractions after treatment with D3T for different incubation times. Each lane contains three pooled samples. (B) Nuclear extracts were isolated from dimethyl sulfoxide (control)-, D3T (10 μM)-, disulfiram (50 μM)-, *tert*-butylhydroxyquinone (tBHQ) (50 μM)-, or β-naphthofalvone (β NF) (20 μM)-treated cells 6 h after treatment. Immunoblot analyses were performed with Nrf2 antibody. A positive standard for the immunoblot was prepared from Nrf2-overexpressing cells (Nrf2 std).

3'), and hematopoietic enhancer of *GATA-1* (5'-GGATCCAAGGAAGAGAG GAC-3' and 5'-TTCCTGGAGGTGACAAAGGG-3').

RESULTS

Nrf2 levels are increased in nuclei and total cellular homogenates by enzyme inducers. Murine keratinocyte PE cells are very responsive to induction of GST and NQO1 activities. For example, NQO1 activity increased fivefold after treatment with 10 μM D3T for 18 h compared to vehicle-treated cells. Therefore, these cells were used to investigate changes in the distribution of Nrf2 after treatment with enzyme inducers by Western blot analysis. Time course studies (Fig. 1A) indicated that Nrf2 levels increased within 20 min of addition of D3T, both in nuclei and total cellular homogenates. At least sixfold increases in Nrf2 were seen after 2-h incubations in nuclear and total cellular homogenate. Basal levels of cytosolic Nrf2 were difficult to detect but appeared to increase slightly after treatment of cells with D3T. Nuclear Nrf2 levels remained elevated for at least 6 h (Fig. 1B). Moreover, treatment with different phase 2 enzyme inducers (D3T [10 μM], disulfiram [50 μM], *tert*-butylhydroquinone [50 μM], and β-naphthoflavone [20 μM]) led to substantial increases in nuclear Nrf2 content compared to vehicle-treated PE cells. Thus, overall levels of the ARE-binding transcription factor Nrf2 increase rapidly and persistently after treatment of PE cells with enzyme inducers.

Inhibitors of protein synthesis and proteasome function affect the accumulation of Nrf2. Accumulation of Nrf2 in PE cells was very sensitive to treatment with the protein synthesis inhibitor cycloheximide (CHX), since the cotreatment of 1 μg of CHX/ml with D3T for 3 h completely blocked both the nuclear and total cellular accumulation of Nrf2 triggered by D3T (Fig. 2A). Treatment with CHX for 1 h prior to addition of D3T also blocked the induction of NQO1 and heme oxygenase-1 activities; products of genes known to be regulated through Nrf2-ARE interactions (data not shown). As shown in Fig. 2A, washout experiments, in which the rate of disappearance of Nrf2 from nuclei was monitored, indicated that the addition of CHX significantly enhanced the loss of nuclear Nrf2. Thus, while continued incubation of PE cells with D3T from 3 to 4.5 h maintained a constant elevation of nuclear Nrf2, removal of D3T from cells at 3 h led to a 50% reduction in nuclear levels of Nrf2 50 min later. Removal of D3T at 3 h coupled with addition of CHX led to a 50% reduction in 30 min and a complete loss of Nrf2 in nuclei within 90 min. Similar results were seen when total cellular levels of Nrf2 monitored. These observations suggest that maintenance of elevated nuclear Nrf2 depends upon de novo synthesis of Nrf2 after treatment with D3T.

Protein degradation also appears to play a role in the regulation of Nrf2. Addition of the 26S proteasome inhibitor, MG132 (15 μM) increased the level of total cellular Nrf2 after incubation of PE cells for 3 h but did not increase the nuclear level of Nrf2 (Fig. 2B). Apparently, Nrf2 is constantly degraded by the 26S proteasome in uninduced cells, such that inhibition of proteasomes causes accumulation of Nrf2 within cells. Presumably, however, there is an excess of Keap1, the cytoplasmic tether for Nrf2, in the cell to keep Nrf2 sequestered in the cytoplasm rather than allowing for nuclear accumulation as its concentration is increased. However, accumulation of both total and nuclear levels of Nrf2 was greatly increased by coincubation of cells with MG132 and D3T, indicating that D3T increases Nrf2 levels in part through a proteasome-independent pathway. Collectively, the effects of CHX and MG132 suggest that levels of Nrf2 protein are regulated through a balance between rapid protein synthesis and constant degradation. D3T treatment may elevate the level of Nrf2 not only by enhanced translocation but also by enhanced protein synthesis.

Levels of Nrf2 mRNA are increased by D3T. The sensitivity of Nrf2 nuclear accumulation to CHX and the additive effect of D3T and the proteasome inhibitor on the accumulation of Nrf2 suggested that transcriptional activation of *nrf2* leading to enhanced synthesis of Nrf2 protein may contribute to the increased level of this transcription factor after D3T treatment. Steady-state mRNA levels of Nrf2 increased ~2-fold 6 h after treatment with D3T (Fig. 2C). mRNA levels returned to basal levels at 24 h, a pattern also observed with nuclear levels of Nrf2 in the liver of mice treated with D3T (27).

Promoter activity of *nrf2* is increased by D3T. The promoter activity of *nrf2* was measured by using a luciferase reporter system to further test the hypothesis that enzyme inducers may enhance transcriptional activation of *nrf2* in PE cells. Chan et al. (5) previously described a 1-kb proximal promoter region for *nrf2*, so this region was isolated by PCR amplification from genomic DNA prepared from the livers of ICR mice. The sequence of the isolated promoter determined here matched the sequence reported earlier. This promoter is very GC-rich and contains several putative AP-2 and SP-1 binding sites. Of particular interest, there are two ARE-like sequences at −754 (AREL2; GCCACAGTCA) and −492 (AREL1; TGACTCC GC) from the transcription start site (Fig. 3A). A full-length promoter construct (pGLNRP−1065/−35) was transiently